MTK 16.

TUDOMÁNYOS BIZOTTSÁG/LEKTOROK
SCIENTIFIC ADVISORY BOARD/PEER REVIEWERS

MŰSZAKI TUDOMÁNYOS KÖZLEMÉNYEK

16.

Szerkesztette / Edited by
BITAY ENIKŐ – MÁTÉ MÁRTON

Prof. dr. Kerekes László
emlékére

TARTALOM

CONTENT

RELONTOUML: DEVELOPMENT OF A MODEL BASED ON RELATIONAL MODEL, ONTOLOGY AND UML

Anita AGÁRDI

University of Miskolc, Faculty of Mechanical Engineering and Informatics, Institute of Informatics, agardianita@iit.uni-miskolc.hu

Abstract

This paper presents a model that combines ontology, UML modeling, and a relational model. The ontology model (and the Ontology Web Language - OWL), UML, and relational model are first introduced in the article. After a review of the literature, the comparison and conversion of the systems are presented. The created model is then presented and a real ontology is modeled using the presented model.

Keywords*: ontology, OWL, UML, relational model.*

1. Introduction

The modeling and visualization of a system is an important task. In the literature, such standard modeling languages are the Unified Modeling Language (UML), the relational database model, and the ontology model. UML (Unified Modeling Language) **[1]** is a standard, general-purpose modeling language. A tool for visually documenting models of large-scale software systems can be used to create textual and graphical models from a variety of perspectives, including: systems, organizations, business, processes, software, programs and databases. They include structural diagrams and behavioural / dynamic diagrams. Structural diagrams refer to the elements of the modeled system. These subtypes are: Class Diagrams, Component Diagrams, Complex Structure Diagrams, Deployment Diagrams, Object Diagrams and Package Diagrams. Behavioural / dynamic diagrams describe what should happen in the modeled system. The following are the subtypes: Activity Diagrams, State Machine Diagrams, Use Case Diagrams and Interaction Diagrams.

Ontology **[2]** is a description of knowledge in a particular area. It contains semantic objects in a given area. One of the best-known languages of ontology is Ontology Web Language (OWL). OWL builds the system from classes - subclasses. An individual is a specific occurrence of a class. Class-es can contain different properties. The property has a domain and range. In the datatype property, the domain is a class, but the range is a datatype, while in the object property, both the domain and the range are a class, so the datatype property associates an entity with a data type, while the object property associates one entity with another entity. The annotation property connects an individual, class, property with an annotation.

The OWL ontology, like the UML and the relational model, has been used in many places, such as health: health ontology systems **[3]**, COVID-19 **[4]**, **[5]**, education: university ontology **[6]**, software technology **[7]**.

Among the database models, the relational model **[8]** is the most common today. The relation is a table. The relation itself is given with a unique name, its rows represent the data. Column names are given with a unique name within the relation, but another relation can contain a column with the same name. The intersection of a column and a row is called a field.

2. RELONTOUML model

In the following, the developed model is presented. The model is based on the relational model, ontology, and the UML model, and called the RelOntoUML model. The goal was to develop a model that is close to the approach of software developers and easy for software developers to

understand. The essence of the model is that it consists of properties from both UML, ontology, and relational models, making it easier to model software systems.

The steps of the transformation are described below, during which the ontology model is converted to the RELOntoUML model.

The ontology uses namespaces; they must be unique names within a namespace. In UML, classes within a package and tables within a database must have unique names [9]. This is converted to the RelOntoUML model as a package, shown in the **figure 1**.
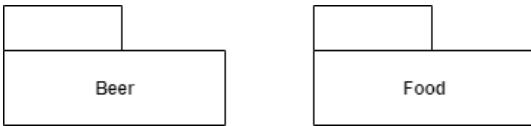
Figure 1. *Namespace (RelOntoUML)*

Classes are descriptors of the system. Ontology classes are simply converted to UML classes [9].
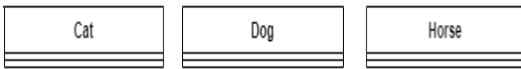
Figure 2. *Classes (RelOntoUML)*

The class-subclass hierarchy is retained in the model. [9]
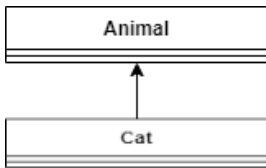
Figure 3. *Subclass (RelOntoUML)*

Individuals are occurrences of classes [9].
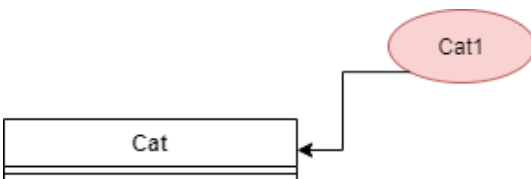
Figure 4. *Individual (RelOntoUML)*

The object property connects two objects, so both the domain and the range are objects.[9]
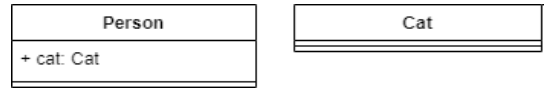
Figure 5. *Object property (RelOntoUML)*

The minCardinality, maxCardinality determines the number of times a class is linked to another class or data type [9].
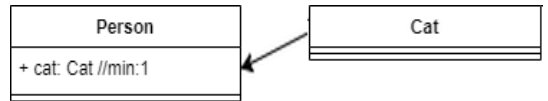
Figure 6. *minCardinality, maxCardinality (RelOntoUML)*

The datatype property associates an individual with a data type [9].
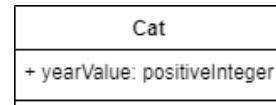
Figure 7. *Datatype property (RelOntoUML)*

A transitive property means that if a property is both (A,B) and (B,C) then it is also (A,C) [9].
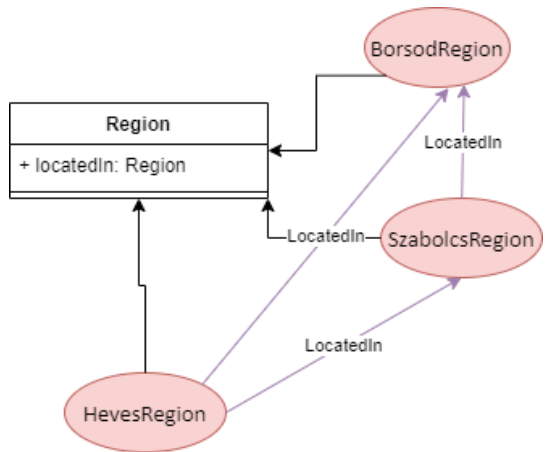
Figure 8. *Transitive property (RelOntoUML)*

A symmetric property in the ontology means that if a property is (A,B), it is also (B,A) [9].
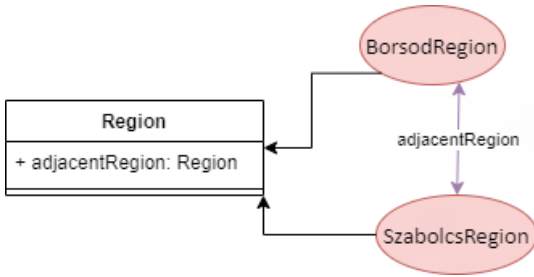
Figure 9. *Symmetric property (RelOntoUML)*

A functional property means that if a property is (A,B) and (A,C), then B = C [9].

Figure 10. *Functional property (RelOntoUML)*

The inverse object property means that one object property is the inverse of the other [9].
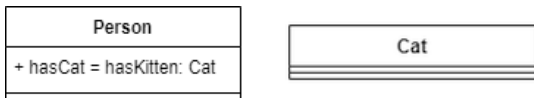
Figure 11. *InverseOf property (RelOntoUML)*

In an ontology, two classes can be created with different names, which, if denoted by the equivalentClass, are equal classes with different names [9].
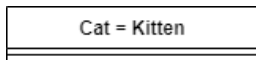
Figure 12. *EquivalentClasses (RelOntoUML)*

In an ontology, you can create two properties with different names, which, if given the equivalentProperty flag, are equal properties with different names [9].
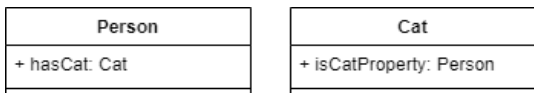
Figure 13. *Eqivalent property (RelOntoUML)*

The sameAs means that two individuals with different names in the ontology are equal [9].
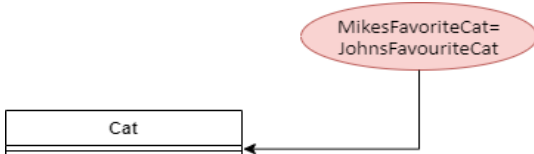
Figure 14. *sameAs (RelOntoUML)*

3. Application of RELONTOUML model on a sample system

SoftwareTechnology [10] is a larger ontology that models software technology. It models software development companies, programming and data description languages, software licenses, platforms (cloud, os), protocols (eg http, ftp) and software product types (eg CMS, CRM).

The ontology models software technology 4 levels with classes and one level with individuals. There are no properties for either individuals or classes.

On the first level is the Thing class, which is the ancestor of all classes in all ontologies. On the second level is Software_Technology. At the third level are the following classes: Software_Company, Software_Language, Software_License, Software_Platforms, Software_Product, Software_Protocol, System_Monitoring. At the fourth level are the following classes: Data_Description_Language, Programming_Language, Cloud_Computing, Operating_Systems, Virtual_Machines, Content_Management_Systems, Search_Engines, Customer_Relationship_Management, Security, Network_Protocol, Security_Protocol .

The ontology also contains a number of individuals. The Software_Company includes the following entities: Adobe, Amazon, Google, Microsoft, Hewlett-Packard, IBM, Oracle, Jetbrains. Data_Description_Language contains the following entities: HTML, XML. The following programming languages are included: C, C ++, Java, JavaScript, Perl, PHP, Ruby.

4. Conclusions

The article presents ontology, relational, and UML models. After the literature of model conversion, the RelOntoUML model was presented, and the transformation of the ontology OWL to the RelOntoUML model. The SoftwareTechnology OWL was converted into RelOntoUML model. The model presents software technology, and its elements such as software company, programming language, license, platform, software product, protocol. The advantage of the developed model is that it provides software developers with easy-to-use modeling. The system created in this way will be well-structured and easy to understand. Another area of research is the conversion of new ontologies to the RelOntoUML model, and possible refinements of the model if required.
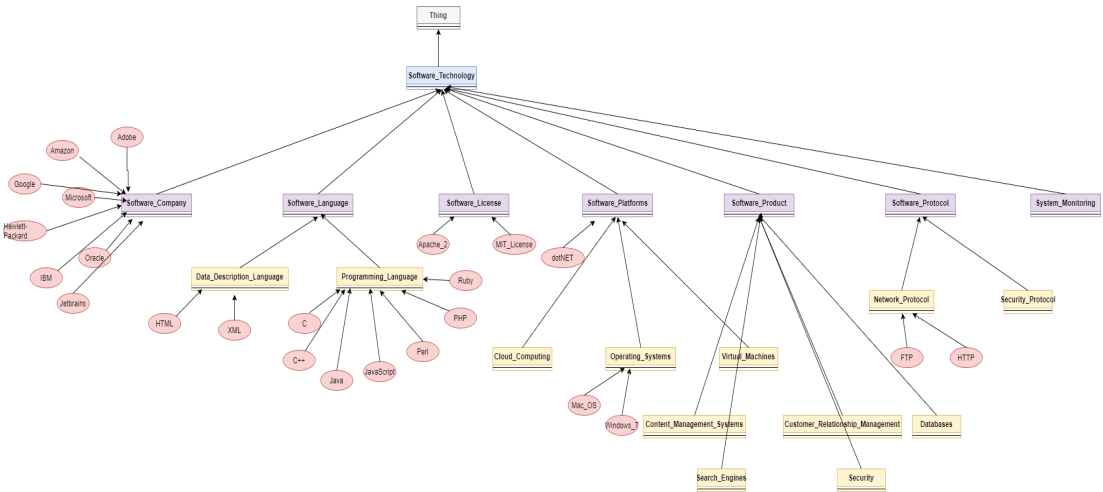
Figure 15. *Visualization of SoftwareTechnology with RelOntoUML*

Acknowledgement

References

[1] Dobing B., Parsons J.: *Dimensions of UML Diagram Use: a Survey of Practitioners*. Journal of Database Management (JDM), 19/1. (2008) 1−18.

[2] Antoniou G., Van Harmelen F.: *Web Ontology Language: Owl*. In: Handbook on Ontologies (2004) 67−92.

[3] Kiong Y. C., Palaniappan S., Yahaya N. A.: *Health Ontology System*. In: 2011 7th International Conference on Information Technology in Asia (2011) 1−4.

[4] Dutta B., DeBellis M.: *CODO: An Ontology for Collection and Analysis of COVID-19 Data*. arXiv preprint arXiv:2009.01210 (2020).

[5] Kachaoui J., Larioui J., Belangour A.: *Towards an Ontology Proposal Model in Data Lake for Real-Time COVID-19 Cases Prevention*. (2020).

[6] Malviya N., Mishra N., Sahu S.: *Developing University Ontology Using Protégé Owl Tool: Process and Reasoning*. International Journal of Scientific & Engineering Research, 2/9. (2011) 1−8.

[7] Gherabi N., Bahaj M.: *A New Method for Mapping UML Class into OWL Ontology*. Spec. Issue Int. J. Comput. Appl.(0975 8887) Soft. Eng. Databases Expert Syst. SEDEXS, (2012) 5−9.

[8] Codd E. F.: *Relational Database: A Practical Foundation for Productivity*. In: *Readings in Artificial Intelligence and Databases* (1989) 60−68.

[9] OWL Guide: https://www.w3.org/TR/owl-guide/ (accessed on: 2021. 11. 09.)

[10] SoftwareTechnology. (accessed on: 2021. 11. 09.) https://github.com/detnavillus/rdf-owl-ontologies.git

sciendo

EME · MTSZ
MTK

MODELLING AND SIMULATION OF THE STRUCTURAL ELEMENTS AND THE OPERATING PROCESSES OF MINING MACHINES

Endre ANDRÁS

University of Petroșani, Faculty ofMechanical and electrical Engineering, Departmen of Mechanical, Industrial and Transportation Engineering, Petroșani, Romania, andrei.andras@gmail.com

Abstract

The paper deals with theoretical bases of the implementation in mining equipment design of up-to-date methods using modelling and simulation, supported by examples of personal research. This has become necessary due to the structural complexity of this equipment, and the variety and aggressiveness of their operating environment. The presented examples refer to different kinds of the equipment used in the mechanical extraction of mineral raw materials, from overall system to working part or tool.

Keywords: *mining equipment, modelling, simulation, design.*

1. Introduction

It is a well-known fact that the structural complexity of the machines and equipment used in mining, along with the variety and aggressiveness of their operating environment, have caused delays in the technological evolution encouraged by the achievements of modern science.

Taking into account the continuous development of technical software specializing in modelling and simulation, there are also a wide range of options for an integrated approach to the mechanical systems of such machines and equipment.

The extraction of mineral raw materials, although based on simple basic operations, requires target-specific machines and equipment. Mining technology, both underground and open pit, is based on three basic operations - wining, - loading/ hauling - cavity support or slope stabilisation.

Mining machines perform the mechanization of these basic operations.

In order to get an image of the large variety, complexity, scale, dimension, weight and sophistication, we present below some examples of typical, up-to -date mining equipment, used for different operations in different technologies, in open pit or underground environments.

Figure 1. presents the main equipment used in open pit coal mining, the Bucket wheel excavator.

In the **Figure 2.** the longwall shearer - loader is presented, used for wining coal in underground mining, by longwall technology. **Figure 3** presents the continuous miner, used in wining coal in underground mining, by room-pillar method. **Figure 4** presents the support shield, used in supporting the cavity in longwall faces.

In the underground mining, in order to reach the mineral reserve, some roadways (tunnels) are headed, with the use of specific machines. **Figure 5** presents the roadheader, for continuous driving, while **Figure 6** shows the drilling jumbo, used in drilling-blasting road driving technology.

We can notice some peculiarity of mining machines due to the fact that mechanization follows the technological process and fits with it, such as:

– increasing the performance requires size and weight growth:

– the moving workplace places machine mobility among the important features;

– each operation requires a separate execution tool;

– a compromise must be reached between specialization and universality.

Figure 1. *Bucket wheel excavator used in open pit coal mines.*

Figure 2. *Longwall shearer - loader.*

Figure 3. *Continuous miner.*

Figure 4. *Longwall support shields.*

Figure 5. *Roadheader.*

Figure 6. *Drilling jumbo.*

2. Modelling of the Load-bearing Structure of the Bucket Wheel Excavators

In the following we present the application of the modelling of the load-bearing structure of the Bucket Wheel Excavator (BWE), and the simulation based on it.

In **Figure 7** is shown the load-bearing structure, namely the boom, which supports the main working part, the bucket wheel (**Figure 8**), and performs the vertical and horizontal motion in order to realize the necessary kinematics.

The modelling and the simulation, is preceded by lab and in situ data acquisition and processing.

The methods based on closed form mathematical formulas or assumptions can give only peak or average values of forces, torques, stresses, power and other parameters. The inconsistency of these data can lead to under or over-dimensioning of the considered parts.

Modeling and simulation technical software makes possible the study and analysis of mechanical phenomena by way of avoiding simplistic hypotheses and closed form equations.

In this approach, the SOLIDWORKS software package was applied on the model of the bucket wheel. Based on the developed model (**Figure 9)**,

Figure 7. *The load bearing structure of the BWE*

Figure 8. *The bucket wheel in operation mounted on the boom*
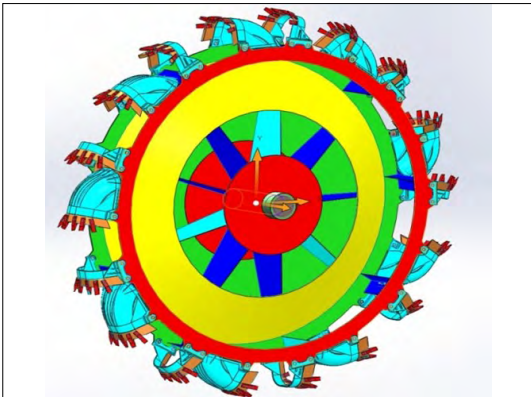
Figure 9. *Detailed modell of the boom.*

Figure 10. *Generating on the model the cutting and loading forces variation in time*
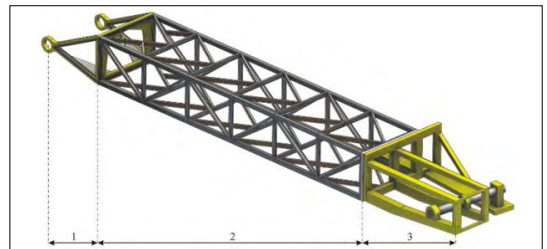
Figure 11. *Detailed model of the bucket wheel.*
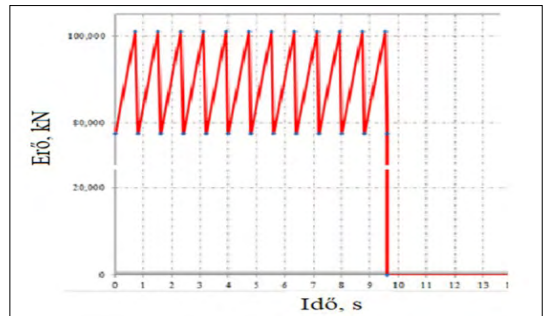
Figure 12. *Resultant force variation during one cut*
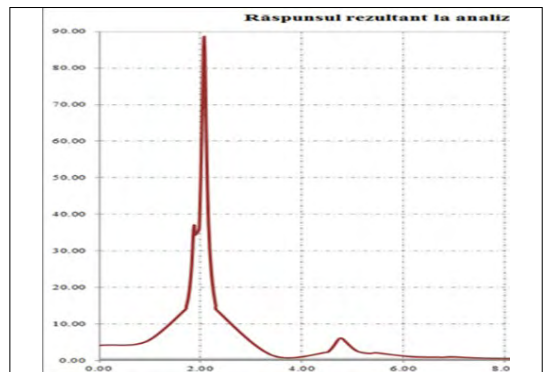
Figure 13. *Frequency response spectrum.*

and knowing the laws of change of the cutting and lifting force values, the variation of the two forces over time was determined (**Figure 10**).

The result of these loads was used as excitation on the boom structure (**Figure 11**) in further simulations (**Figure 12**).

Thus, for example, we examined the vibrations of the boom structure. Some of the results are presented in **Figures 13** and **14.** They are the same as the results obtained by the measurements.

Data was processed with the use of two procedures. The modal analysis was completed by taking into consideration a global damping coefficient. On the other hand, the response function analysis was performed by taking into account the Rayleigh's damping coefficients. Both showed that the maximum deflection corresponds to the frequency of 2.07 Hz. Since the excitatory frequency is 1.25 Hz, resonance phenomenon may be avoided with a consistent probability.[1, 2].

3. The modelling of the energy and power demand of the Bucket Wheel Excavator

Based on the model of the excavator, we have developed a new method for calculating the energy and power needs of Bucket Wheel Excavator. [3]

Using CAD, the method presented determines the amount of rock extracted during swinging (**Figure 15**). Knowing the specific energy demand, we calculated the energy and performance parameters.

The results shown acceptable deviations from the values calculated by the traditional method. Since the proposed method is based on numerical calculations, it can be applied to any BWE, among various rock-types and working place parameters.

4. Modelling of the working tool of the Bucket Wheel Excavators

The benefits of modelling are also highlighted by the optimization of the sizing of the tooth which is the working tool of the bucket. [4]

Thus, knowing the forces acting on the tooth, using the finite element method and numerical modelling, we established the optimal shape.

The results are shown in **Figures 16** and **17**.

5. Conclusions

The recent advances in modelling software offer a wide range of options for an integrated approach to the design of mechanical systems of mining machines and equipment, by modelling and simulation.

Using the SOLIDWORKS software package, we have developed a model of the bucket wheel. Based on this model, we have performed different simulations, from overall system to working parts and tools.
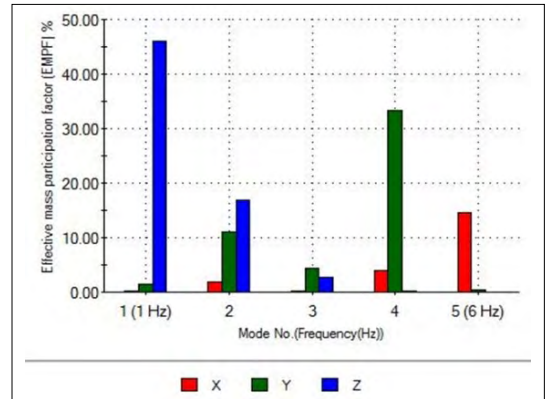
Figure 14. *Frequency response diagram.*
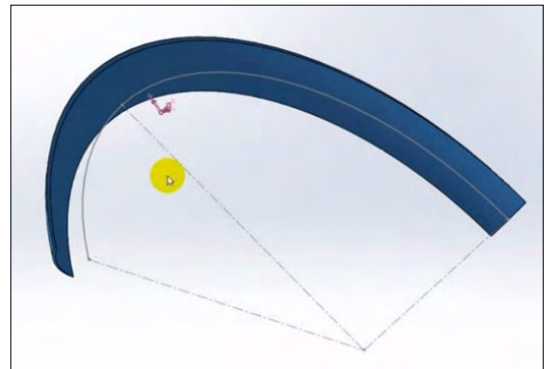
Figure 15. *The volume of cut during one swelling of the boom.*
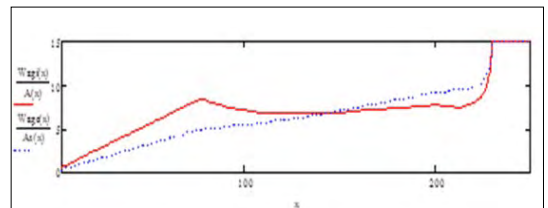
Figure 16. *Optimal shape of the tooth's longitudinal cross section obtained by analitical modelling.*
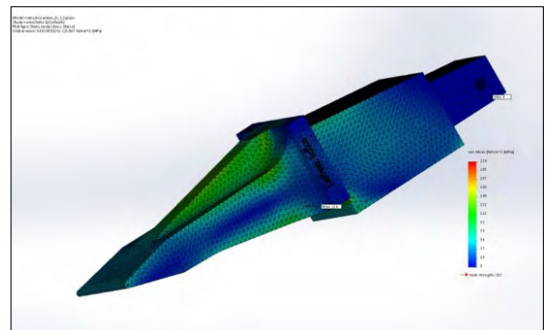
Figure 17. *Optimal shape of the tooth by FEM.*

References

[1] Popescu F. D., Radu S. M., Andras A., Brinas I : *The Modal Analysis, Using Simulation And Modelling, of The Boom of The Erc-1400 Bucket-Wheel Excavator During Operation.* Acta Technica Napocensis Series-Applied Mathematics Mechanics And Engineering, 63/4. (2020) 353−362.

[2] Popescu F. D., Radu S. M., Kotwica K., Andraş A., Brinas I., Dinescu S.: *Vibration Analysis of a Bucket Wheel Excavator Boom Using Rayleigh's Damping Model.* New Trends in Production Engineering, 2/1. (2019) 233−241.
https://doi.org/10.2478/ntpe-2019-0024

[3] Brinas I., Andras A., Radu S. M., Popescu F. D., Andras I., Marc B. I., Cioclu A. R.: *Determination of the Bucket Wheel Drive Power by Computer Modeling Based on Specific Energy Consumption and Cutting Geometry.* Energies, 14/13. 2021.
https://doi.org/10.3390/en14133892

[4] Andraş A., Andraş I., Tomuş O.B.: *Optimization of Geometric and Strength Parameters of Teeth for Bucket Wheel Excavator in View to Increasing the Cutting Efficiency.* 17th International Multidisciplinary Scientific GeoConference, SGEM 2017. 607−612.
https://doi.org/10.5593/sgem2017/13/S03.077

sciendo

EME • MTSZ
MTK

NEW TRENDS IN MINING EQUIPMENT DESIGN

József ANDRÁS,[1] József KOVÁCS,[2] Endre ANDRÁS[3]

[1] University of Petrosani, Faculty of Mechanical and electrical Engineering, Department of Mechanical, Industrial and Transportation Engineering, Petrosani , Romania, iosif.andras@gmail.com

[2] PUniversity of Petrosani, Faculty of Mechanical and electrical Engineering, Department of Mechanical, Industrial and Transportation Engineering, Petrosani , Romania, kovacsi@mail.com

[3] University of Petrosani, Faculty of Mechanical and electrical Engineering, Department of Mechanical, Industrial and Transportation Engineering, Petrosani , Romania, andrei.andras@gmail.com

Abstract

Mining machinery and equipment have changed little in recent decades, from the point of view of the principle of operation, construction and structure. But in terms of dimensions, performance and stresses they have made a lot of progress, experiencing unprecedented sophistication and complexity. In order to fulfil the new requirements imposed by the increasing productivity and efficiency demands, as well as the economic, environmental and safety constraints, their design and development must comply with the general advance of overall technology. Therefore, recently, modern analytical methods have also been included in the design and development of mining machines. Among other issues, the present paper examines the theoretical and conceptual aspects related to the mining machinery' design requirements involving mechatronics.

Keywords: mining machinery, engineering design, mechatronics.

1. Introduction

Throughout the history of mankind, mining has had a significant impact on general social and economic development. Many ground-breaking technological innovations, such as steam engines and pumps, are associated with the golden age of mining. In the following eras, mining, as a supplier of raw materials, has applied the results of technological developments such as compressed air, electric motors, hydraulic drives, etc., contributing through this to their further development.

The current relative stagnation of mining has been caused by severe economic, financial and environmental limitations. In spite of this, mining remains an essential procedure in the supply of energy and basic raw material.

In the present the "green energy" hysteria has cornered coal-based energy production, but "renewable energy" resources carry a potential energy and critical mineral need-induced crisis that we are not yet able to handle.

For this reason, in the near future, mining can expect a new boom, instead of recession.

At the beginning of the third millennium, mining technologies, equipment and technical solutions reached a certain maturity. This can be considered as the trigger of an emerging revolutionary jump that cannot be ignored.

The unprecedented development of manufacturing technologies is supported by the boom of electronics, fine mechanics, automatic control and computing. Its results were incorporated more easily and efficiently in other industry branches. This caused a lag in the development of mining machinery compared to industrial areas at the forefront of technological development.

As a consequence, design and development methods in mining were positioned later on a scientific basis. [1]. So, the development of technologies and equipment used in mining present slower progress compared to other industrial branches.

In order to overcome these phenomena, it is necessary to find new solutions for updating knowledge and technological development. It is also necessary to mention here that mining technology development has always resulted from a symbiosis of creativity and traditional solutions. Due to this, innovation in mining presents special peculiarities [2].

Knowing that mining technology is based on three basic operations - wining, loading-hauling, and supporting, the mechanization of these has sometimes evolved independently of each other, none-the-less influencing each other.

A notable peculiarity of the development of mining technologies is that the explosive evolution of one component leads to the rapid development of the other two components. This evolution is cyclical, resulting in the eventually emergence of an entirely new technology.

There exist examples where the development of mechanization requires a new technological process: a significant one is the use of tunnel boring machines (TBM). The fact that mechanization follows and fits the technological process, is another peculiarity of mining machines. Increasing performance requires size and weight increase. The moving workplace requires that the mobility of the mining machine is one of its important features. In some cases this implies that the three operations (functions) require separate execution tools.

The functionality of a particular machine derives from the integration of the assembly of each functional element and the correlation of functionalities [3, 4].

Consequently, the functional analysis is essential for the design of equipment. Based on this, important conclusions can be drawn on the specifics of mining machines and equipment, as well as on the functionality-design interaction.

Thus, when designing a machine, it is necessary to consider the types of interconnections through which functional elements are connected to the whole machine system, as well as the degree of integration of the machine or functional elements into the system.

As the integration between the elements of the equipment (technical system) is higher, the peculiarity of the equipment for certain conditions of use is greater, the degree of versatility is lower, which requires an optimal compromise between specialization and universality.

Depending on the degree of integration of functional elements into different systems, it can lead to new structural restrictions dictated by the compatibility of functional elements, and the need to perform some new secondary functions may entail changes in structure.

Therefore, the design of any functional element, be it a unique machine or an integrated system, should be carried out in a systemic context, taking into account the effect of the connection of the given element with the others on its functionality (operation in accordance with the requirements). At the same time, the expected stresses, known only in average or maximum values, which can be attributed to the random nature of workflows such as wining, loading, haulage, support, (might) lead to oversizing of the structural components.

2. Mechatronics as a design approach

Traditional design of mining machines manages separately the structural-functional parts (mechanical, electrical, hydraulic and control units).

Mechatronics, as a design approach, can offer an innovative procedure for the systematic design of mining machinery and equipment.

The multidomain nature of these machines, in traditional design, may lead to the impossibility of optimal alignment of the structural and functional parts of different varieties. The loads of mining machinery usually result from the prescribed motion of the executive element while it interacts with the working environment.

The traditional mechanical design basically tries to compute the trajectories, velocities and accelerations of parts, in the condition of action of a known force system. (Figure 1)
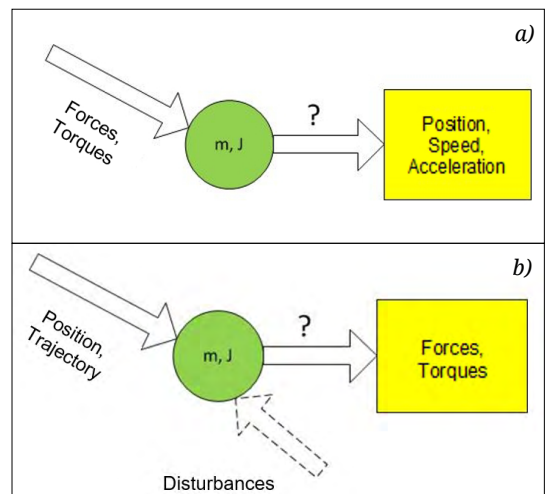
Figure 1. *Traditional (a) and mechatronics based (b) design approach.*

In mechatronics, mechanical systems are also essentially complex, but in contrast to the previous one, the subject of the computing becomes the forces and torques needed to maintain a prescribed trajectory, speed and acceleration of the parts. The computed values are provided by continuous measurement-based control. (**Figure 2**)

Figure 3 refers to the distribution and treatment of flows (energy, material and information) used in mechatronic design. **[5, 6]**.

The processing of information refers to the fact that the operating parameters of mining machines should generally only be adapted to rock cutting factors known in average terms, together with compliance with geometric, desired shape, productivity and energy requirement limitations.

These requirements are imperious for all kind of rock cutting machines, but specially for roadheaders. However, since the direct perception of the different parameters is impossible or in principle complicated, they can be obtained indirectly from the operating parameters only by calculation. Therefore, a drive is required with a complex structure containing embedded sensors for mobile elements. Up to date artificial intelligence methods (fuzzy logic or neural networks) may be used for calculations.

The experimental system developed by Polish researchers **[7]** is shown in **Figure 4**. The data of the boom and of the loader plate position sensors are processed by the control unit which properly regulates the parameters of the milling head and loading system.

All this together uses data from the milling head drive torque and the boom swing speed sensors for optimal energy use and productivity, observing the requested shape of the cross section of the cut.
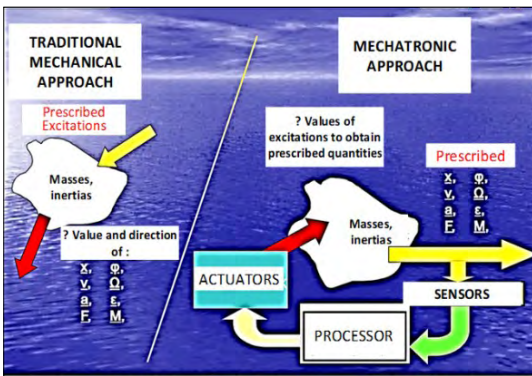
Figure 2. *Comparison of traditional / mechatronic design.*
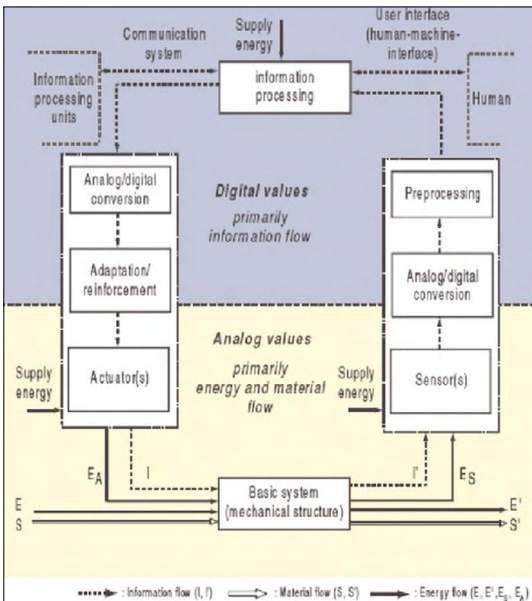
Figure 3. *Flows used in mechatronic design*
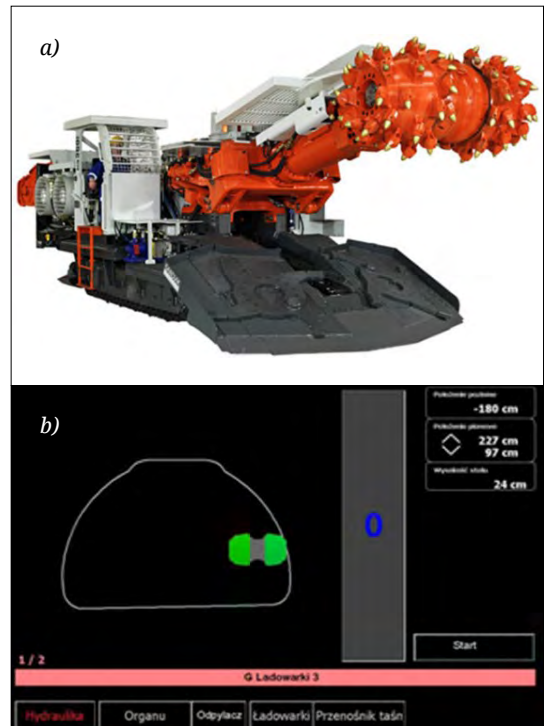
Figure 4. *Roadheader designed on the basis of a mechatronic approach, (a) display screen observing the shape of the cross-section of the cut (b).*

Another example also applies to drilling carriages (jumbos) used in cutting drives (**Figure 5**) which are an essential tool for drilling-blasting technology.

In this case, compliance with the prescribed drilling scheme (**Figure 6.a**) is the main issue. The appropriate position of the drill rod end and the direction of the conductive rail (**Figure 6.b**) for each borehole is calculated on the basis of data from built-in sensors and made by the displacement of the hydraulic actuators. With the help of a software, one can display the state of the process on a screen(**Figure 6.c**).

3. Conclusions

Modern analysis methods have recently been used in the design and development of mining machines.

They are not just tools, but rather an approach.

The specificity of mining machinery allows to fulfil this requirement under certain conditions.

The multidomain nature of these machines, in traditional design, may lead to the possibility of optimal alignment of the structural and functional parts of the separate parts.

Mechatronics as a design approach can offer an innovative approach to the regular design of machinery and equipment used in mining, which has been illustrated by examples.

References

[1] Spies K.: *Limits of Further Development of Technologies of Underground Coal Extraction and the Methodological Procedure in Systematic Search for New Technologies*. Zeszyty Naukowe Politechniki Śląskiej, Górnictwo.
https://delibra.bg.polsl.pl/dlibra/publication/46951/edition/42857/content

[2] Andraș A., Andraș I.: *Applications of Artificial Intelligence and Mechatronics in Mining Equipment Development.* Annals of the University of Petroşani, Mechanical Engineering, 17. (2015), 5–20.

[3] Andraș A., Andraș I., Kovacs J., Tomuș O. B.: *Monografia Problemy transportu i przeróbki w górnictwie. Modelowanie procesów. Artificial Intelligence, Mechatronics and Robotics in Mining Equipment Development* (2015). Akademia Górniczo Hutnicza, Krakow, 134–149,

[4] Andraș A.: *Ingineria proiectării echipamentelor pentru industria extractivă.* Editura Universitas, Petroșani, 2014.

[5] András J., Kovács J.: *A műszaki innováció sajátosságai a bányászatban (Specificity of Innovation in Mining).* Műszaki Tudományos Közlemények, 4. (2016) 23–26.
https://doi.org/10.33895/mtk-2016.04.02

Figure 5. *Drilling jumbo*

Figure 6. *The prescribed drilling scheme (a), the boom with the conductive rail (b), the display screen (c).*

[6] András J., Kovács J.: *A mechatronika alkalmazása a bányagépek tervezésében (Implementing Mechatronics in Mining Equipment Design).* Műszaki Tudományos Közlemények 1. (2014) 39–42.
https://doi.org/10.33895/mtk-2014.01.02

[7] Cheluszka P. : *Numerical Studies of the Dynamics of the Roadheader Equipped with an Automatic Control System during Cutting of Rocks with Different Mechanical Properties.* Energies, 14(21) (2021) 7353;
https://doi.org/10.3390/en14217353

sciendo

EME • MTSZ
MTK

STRATEGIC PLANNING AND PERFORMANCE MANAGEMENT FOR CITIZENS OF HARGHITA COUNTY WITH THE INTRODUCTION OF THE CAF BASED QUALITY MANAGEMENT TOOL (CAFHR) PROJECT

Imre ERDŐSSY,[1] László KEREKES,[2] István SZŐCS[3]

[1] *ConsAct Kft., Budapest, Hungary, eimre@outlook.hu*

[2] *Bogdan Voda University, Faculty of Economics, Management. Cluj-Napoca, Romania*

[3] *Harghita County Council,. Csikszereda., Romania, szocsistvan@hargitamegye.ro*

Abstract

The Harghita County Council has decided to carry out a self-assessment to evaluate the adequacy of its processes in the framework of a complex organizational development project using the CAF (Common Assessment Framework). The outcome of the performed self-assessment showed the capabilities and results of the operation, as well as the tasks of ensuring short- and medium-term development. This article aims to point out the needs and possibilities for improving administrative processes by presenting the experiences of the project. An important experience of the project is to prove the necessity of taking into account the specific features in addition to prove the general applicability of the model.

Keywords*: CAF, Quality management, Harghita County Council.*

1. An organization-wide performance tool – introducing the CAF model

The Common Assessment Framework (CAF) is a complete quality management tool developed by public sector representatives for the public sector on the basis of the European Foundation for Quality Management (EFQM) Model of Excellence. It was prepared at the request of the heads of directors (directors-general) responsible for the development of the civil service in the Member States in cooperation with the so-called Innovative Public Service Working Group of quality professionals. CAF promotes performance and efficiency-oriented quality development in public administrations using state-of-the-art quality management techniques. The model is simple, easy to use and provides a suitable methodological framework for self-assessment of public administration.

The CAF is designed to be used in all areas of the public administration sector, applicable in all organisations at national/federal, regional and local levels. It can also be used within wide variety of circumstances, e.g. as part of a systematic development programme or as a starting point for development work within a given organisation.

The application of CAF provides an appropriate framework for an organisation to start a continuous development process. Here's how it helps:

– evidence-based evaluation, based on a set of criteria widely accepted in the administrative sphere of European countries;
– the establishment of outstanding levels of progress and performance;
– developing consistency of governance and reaching consensus on what needs to be done to develop organisations;
– the relationship between the different achieved results and the practical solutions or capabilities to be supported;
– the involvement of staff in the development process;
– promote the development of good practice solutions and the possibility of sharing them between different areas within the organisation and with other organisations;

– the integration of different quality initiatives into everyday workflows;

– timely measurement of progress through periodic self-assessments.

It is based on the assumption that excellent results in terms of organisational performance, citizens/clients, people and society can be achieved through management-led strategy and planning, staff, partnerships and resources, as well as through processes. This tool examines the organization from several different perspectives at the same time, and analyses organizational performance using a complete approach.

The main requirement for the model, therefore, in the development process was to be appropriate to the framework and applicable to public administrations, taking into account their specificities and compatibility with other organisational models used in European public administrations.

From the user's point of view, it is important to meet the aforementioned requirements for two reasons: firstly, because most quality systems were developed in the economic sphere and market organisations, therefore the CAF model takes particular account of administrative specificities. On the other hand, it is also important that it can be combined with quality systems, used in the private sector, in particular EFQM, and by methods, in order to present the results from the field of quality management to the public sector.

The model itself is not a quality management system, but a management tool that can be used to define development goals that make the operation of the organization more effective, and also to develop the organizational culture by the self-evaluation process.

The model is related to the requirements of the ISO 9001 standard system in its approach and principles, but differs significantly in content and method. While ISO 9001 is a management tool based on regulation and continuous development, which has a direct impact on the operation of the organization, CAF primarily means continuous organizational performance evaluation and has only indirect influence on the activities of the public administration organization. CAF imposes requirements in the examination of the different areas of operation, leaving the evaluation of the achieved results to the organization.

The CAF is based on the principle that the "level of performance" of an organization depends on the proper management of the five areas of operation. These areas are:

1. management,

2. strategy-making and planning,

3. staff,

4. partnerships and resources,

5. processes.

Excellence should also be assessed in relation to the results of the organization from several perspectives:

6. performance of the organisation (objectives established),

7. perspective of citizens/customers,

8. point of view of the staff,

9. social impacts.

CAF self-assessment is based on a complete approach to the analysis of organizational performance, covering all elements of the system as a whole, since the organisation must be examined at the same time from different perspectives and criteria for both the operation and the results of the organisation.

1.1. Purpose of the CAF

CAF is an easy-to-use tool to help public administrations across Europe, apply quality management methods and processes, to improve performance. CAF provides a self-assessment framework, similar in concept to larger TQM models, in particular the EFQM model, but specifically designed for public administrations, taking into account the differences between them.

CAF is a 'public domain' tool that is accessible to all free of charge and is easy to learn. Moreover, it helps European public sector organisations (hereinafter referred to as 'public service organisations') to use quality management techniques to help them improve their performance. The CAF model is designed to be applicable to all public sector organisations at European, nation-state, regional and local level.

CAF supports the entire development process within the organisation and sets out five main objectives:

– the introduction and dissemination of a culture of excellence and the principles of the TQM in public service organisations;

– the gradual implementation of organisations throughout the PDCA development cycle;

– facilitating the self-assessment of public service organisations in order to identify errors and identify the necessary development measures;

– the creation of bridges between the various models used in quality management, both in the private and public sectors;
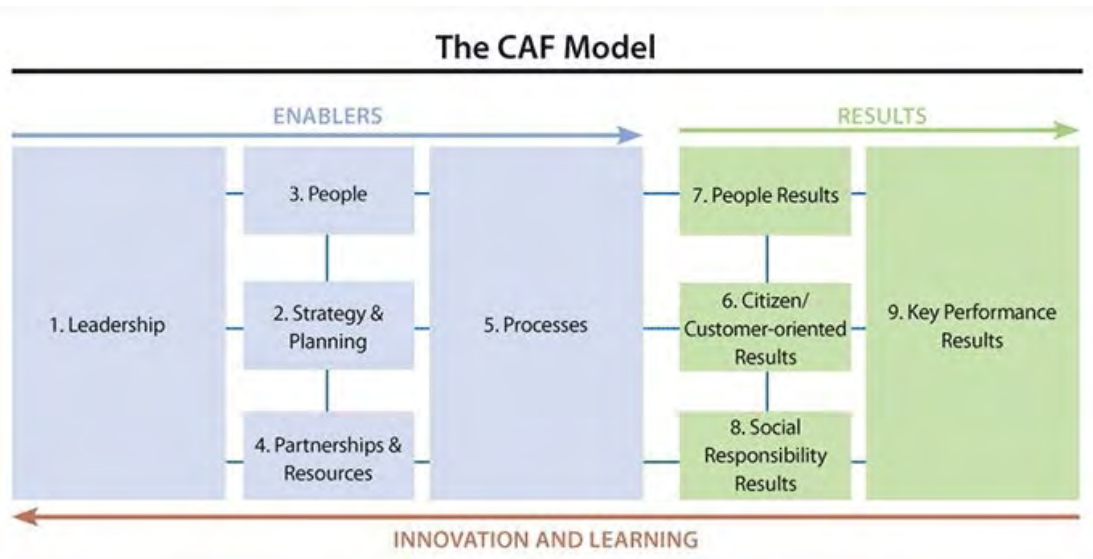
Figure 1. *Model CAF 2013*

– enabling and supporting bench learning between public service organisations.

Organizations that aim to strive for superior performance and that want to localize a culture of excellence are starting to apply the CAF model. Over time, the effective application of CAF can lead to the further development of this kind of culture and way of thinking within the organization.

1.2. Model CAF 2013

The nine-element structure of the CAF model, shown in Figure 1, includes the main aspects that must be taken into account in any organizational analysis. Criterion 1-5, the so-called "Capabilities", takes into account the practices of organization management. These criteria determine what the organization does and how it solves its tasks in order to achieve the desired result. Criteria 6-9 presents "Results" in the areas of citizens/clients, staff, social responsibility and key performance of the organisation, based on personal opinions, personal assessments and performance measurements on the other hand. Each criterion consists of several sub-criteria (The 9 criteria contain a total of 28 sub-criteria.)

The 28 sub-criteria define the main aspects to be taken into account in the evaluation of the organization. Examples explaining the content of the sub-criteria are illustrated in detail in [2], which also suggests the possible areas for determining the organization's compliance with the require-ments of the sub-criteria. The examples show a lot of good practice from all over Europe, but they are not applicable to all organisations, but they are still suitable for guiding.

The criteria and sub-criteria in the questionnaire cannot be changed, but the examples can be tailored to the organization, expanded and narrowed due to a better understanding. (The Harghita County Council has completed a questionnaire tailored to the self-assessment of the organization.)

Incorporating the conclusions drawn from the evaluation of the results into management practice ensures the continuity of innovation and learning cycles that accompany an organisation on the road to excellence.

1.3. How to use CAF 2013

As explained above, the structure of the criteria and sub-criteria should not be modified, since this structure ensures that self-evaluation covers the functioning and results of the organization in all areas and in all aspects. At the same time in examples related to sub-criteria, it is permissible and important to interpret them and adapt them to the organization.

In Harghita County Council (HCC), a questionnaire tailored to the organization was completed, using a 'traditional scoreboard'. In general, the "traditional" CAF assessment assesses all sub-criteria at the level of the PDCA cycle

1.4. The "CAPABILITIES" side (1-5) criteria evaluation

The PDCA principal assessment method is based on the fact that the point values are determined on the basis of where the measures are in place during the implementation phase and not on the basis of the number or weight of the implemented measures. The questionnaire respondents score according to their subjective feelings. The assessment used can be seen below:

Table 1. *Scores used in the evaluation of the "CAPABILITIES" (1-5) criteria*

Level	Description of levels related to capabilities	Score
–	If the organization does not perform the activity set out in the sub-criteria or does not intend to introduce it, then 0 points; if the idea of the introduction has already been proposed, but the design has not started, the value that can be given is around 10 points.	0–10
Plan	There are only plans to develop the applicable practice.	11–30
Do	The sub-criteria area of the organisation is operated as planned, but the experience has not yet been evaluated.	31–50
Check	In the area related to the sub-criteria, the evaluation of the operation is carried out regularly, but the results of the evaluation have not yet been put into practice by the organization.	51–70
Act	The organisation develops its operations on the basis of sub-criteria-related audits and reviews.	71–90
PDCA	The organization systematically (planned and regularly) uses methods of continuous development in the area related to the sub-criteria. It also incorporates the results of benchmarking and learning from each other into the development.	91–100

1.5. Evaluation of the "RESULTS" criteria (6-9)

In summary, self-assessment according to the CAF model gives the organization the opportunity to learn more about itself. The goal of CAF is to hold a mirror to the organization to judge its performance.

Compared to a complete quality management model, CAF is designed to be a very user-friendly model. Any organization that wants to go further will choose one of the more detailed quality management models. CAF has the advantage of being compatible with these models, and this can be the first step for an organization that wants to move forward in quality management.

Table 2. *Scores used in the evaluation of the "RESULTS" side criteria (6-9)*

Evaluation of results	Score
There are no measurable results or relevant information related to the sub-criteria.	0–10
The results are measurable, their evolution over time is deteriorating and/or the results do not achieve the objectives set by the organisation in relation to the sub-criteria.	11–30
The results stagnate and/or in some cases have achieved the organisation's objectives in relation to the sub-criteria.	31–50
The results show an improving trend and/or most of the objectives set are met in relation to the sub-criteria.	51–70
The results show a significant improvement and/or all objectives set are met in relation to the sub-criteria.	71–90
The results are excellent and kept constant, all the set goals related to the sub-criterion are met. Important indicators for the sub-criteria show positive results compared to the results of other organizations.	91–100

2. Project plan for the 2021 organizational self-assessment carried out by Harghita County Council in accordance with the CAF methodology

Within the framework of the project "Strategic planning and performance management for the benefit of Harghita County citizens through the introduction of the CAF-based quality management tool" (CAFHR), HCC council has set itself the goal of organizational development of the council.

During the implementation of the project, HCC decided to introduce a CAF survey, which has been a reliable organizational level performance measurement and self-assessment tool in the European public administration for many years.

By conducting the survey, the aim of HCC is to identify and evaluate the problems inherent in the organisation's activities which affect its efficiency and effectiveness, by examining the criteria set out in the CAF. On this basis, the council may determine its own organisational strengths and weaknesses and develops and implements measures to improve its performance. CAF's repeated annual/biennial audits also provide an opportunity to monitor and compare changes in

employee perceptions of organisational capabilities and performances in a timely manner.

The CAF self-assessment was carried out by HCC for the first time this year.

2.1. Planning the self-assessment project

In connection with the organizational development project, on the HCC senior management a decision has been taken to carry out a self-assessment according to the CAF.

This decision reflected the intention of managers to be actively involved in the process, i.e. to recognise the added value gained through self-assessment and to guarantee that they will have an open attitude, accept results and be ready to make improvements based on them. This included their commitment to providing the resources needed to carry out professional self-assessment.

A high degree of commitment and a shared responsibility from senior management and staff is a key to the success of the self-assessment process in the council.

The HCC involved an expert contributor to this task, who played a key role in the collection and processing of data and information and in the preparation of the report.

During the planning work, the Management of HCC defined the focus and method of self-evaluation. According to this, it was decided:
– that self-assessment covers the whole organisation,
– that self-assessment is applied using the traditional scoring table;
– the evaluation is carried out online.

The senior management decided on the project manager and appointed Mr. István Szőcs – general manager of Management division to the task, who has years of organizational knowledge and experience. His duties included:
– detailed planning of the self-assessment project together with the related communication tasks;
– consultation and communication with all stakeholders;
– organisation of the training of the self-assessment group;
– organising the collection of supporting materials and evidence to support self-evaluation;
– support in setting development priorities and developing development programmes.

Because the language and examples used in the CAF model were foreign and too far from daily practice to be used directly, the "Counselling" of the questionnaire, i.e. its adaptation to the organisation, has been carried out.

2.2. Communication of the self-assessment project

Communication was primarily the responsibility of the project manager. Communication has played a significant role because it has covered all stakeholders involved in the project, in particular middle managers and staff. HCC managers understood that if communication about self-assessment goals and self-assessment activities is not clear, it is likely that self-assessment will only be considered by staff to be another task issued by management and "ticked off". The risk is the reluctance of the participants, who must be fully committed and active in the process for the project to succeed.

Communication focused on ensuring positive results for the whole organization, as well as for citizens and customers, by conducting the self-evaluation process. The project manager stressed the following:
– why it matters whether the organization performs self-evaluation;
– why this has now gained importance for the organisation;
– how self-evaluation and its results relate to the strategy of the organization;
– how self-evaluation relates to other general developments in the organization, such as the ongoing transformation programme in the organization.

2.3. Create a self-assessment group/project group

The self-assessment group was set up in a representative manner in the organization, all units, all functions and all levels of the organisation were sufficiently represented. When determining the number of the self-assessment group, the CAF methodological recommendations were taken into account.

The total number of persons in the organization is 217 and its organisation consists of 8 larger units, therefore 60 people were invited to carry out the self-assessment. During the self-assessment period, 44 people self-assessed as a result of the application of holidays, sick leave or other verified absences, as well as the principles of anonymity and volunteering, thus providing the necessary answers for the interpretation of the data.

The self-assessment group/project group was supported and assisted by the project manager

and a working group appointed by a presidential decree, if there was a disruption in the online login or the completion of the questionnaire, in interpreting a question.

2.4. Realization of self-assessment

Each member of self-assessment team, 44-persons, had to give an accurate assessment of the organisation for each sub-criteria, using the documents and information provided by the project manager. This assessment was based on individual knowledge and work experience within the organisation, as well as related facts. However, regular discussions and communication between each other and with other colleagues were typical during the filling period.

As a first step, in light of the facts revealed, the existing strengths and areas to be developed were formulated in a concise manner, and at the end, based on their findings, the individual sub-criteria were assessed numerically on the basis of the 'traditional' scoring table.

Justifications could also be added to individual assessments, which included:
– interpretation of the strengths identified and areas for improvement,
– interpretation of the numerical assessment if it is to be explained on the basis of the textual assessment.

During the course of completing the questionnaire, the project manager was available throughout and handled questions from the members of the self-assessment team during the individual evaluation.

3. Presentation of the results of self-assessment

As a typical self-assessment report, the Harghita County Council's self-assessment report follows the CAF structure and includes the following elements: strengths and areas to be developed for each sub-criteria, supported by the related evidence and justification.

This data is available to management as background information and sufficiently supports progress in the self-assessment process. After processing these data, leadership presentation was made on the following:
– summary and analysis of the textual and numerical results of the self-assessment,
– highlights of the strengths of greater importance and areas for improvement;
– identification of the strengths and areas to be developed that can be easily and quickly achieved, resulting in rapid success;
– proposal of measures in the areas of priority development,
– proposal of further steps related to self-assessment.

3.1. Presentation of numerical results and comparison with benchmark data

Figure 2 and **3** illustrate how HCC values are based on the following criteria from Table 4 (Partnerships and resources), in criterion (Results of customer-oriented operation), (Social impacts) and (Performance effectiveness) exceeded the organisational average. For criterion 3 (Human
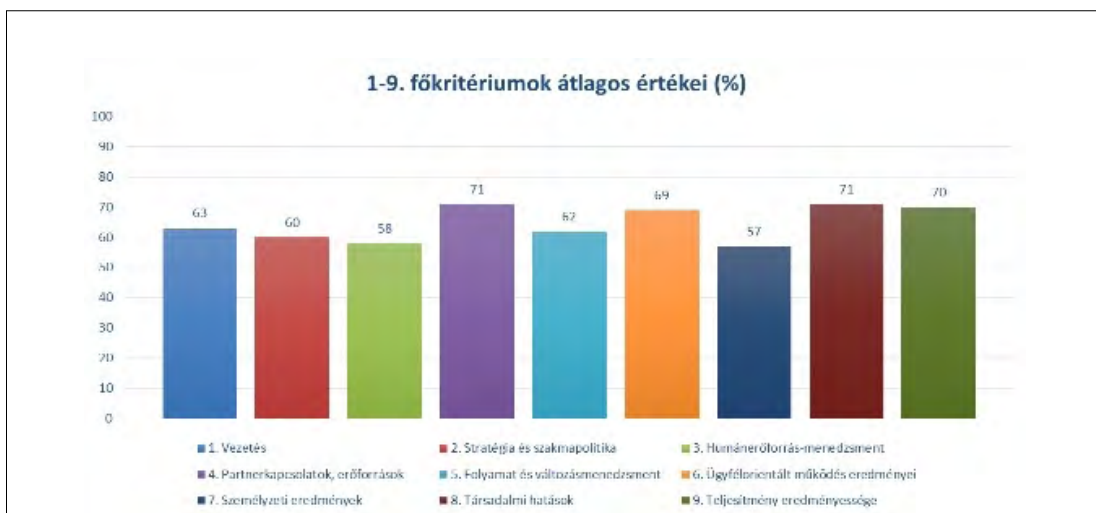
Figure 2. *Average scores for main criteria 1-9* **[2]**

Figure 3. *Standard deviation of point values for main criteria 1-9* **[2]**

resources management) and criterion 7 (1) (a) and (b) (Staff results /employee satisfaction/) the results were below the average.

The organisational average of the criteria is 65 %.

In the table below, the average of HCC data with the average of 1235 surveys in Hungary was compared. The data of Harghita County Council are in brackets.

From **Table 3.** it can be seen that the results of the Harghita County Council are above the Hungarian national average for all criteria. Significant differences are in the main criteria 4. (Partnerships, resources) and 8(1)(a) and (b). (Social impacts).

For sub-criteria, underperformance is shown in 3.3, 4.1, 4.4 and 5.2..

Table 3. *Comparison of HCC self-assessment results with benchmark data* **[2]**

		Criteria								
		1.	**2.**	**3.**	**4.**	**5.**	**6.**	**7.**	**8.**	**9.**
Sub-criteria	**1.**	58 (62)	60 (69)	53 (64)	63 (59)	60 (69)	64 (70)	54 (58)	59 (71)	63 (71)
	2.	60 (62)	57 (59)	54 (55)	64 (74)	64 (51)	64 (67)	53 (55)	58 (69)	62 (70)
	3.	56 (56)	56 (60)	55 (50)	65 (69)	60 (70)	-	-	-	-
	4.	61 (72)	56 (53)	-	61 (58)	-	-	-	-	-
	5.	-	-	-	54 (57)	-	-	-	-	-
	6.	-	-	-	58 (77)	-	-	-	-	-
Average		59 (63)	57 (60)	54 (58)	61 (71)	61 (62)	64 (69)	54 (57)	58 (71)	62 (70)

3.2. Strengths and areas to be developed

In assessing the results of the 2021 organizational survey - in accordance with general practice - when determining organisational strengths and weaknesses, the starting point was the organisational average established for Harghita County Council as a whole. Those properties and results whose mean value deviated by at least 6.5 percentage points from its 65% value were included. The following formula can therefore be used:

organizational weaknesses < 58,5%–71,5% < organizational strengths

This formula provides an opportunity to identify organisational strengths and weaknesses at both the level of the main and sub-criteria and the individual indicators, which is one of the basic objectives of the CAF survey.

Table 4. I*dentifying areas to be developed within the HCC's self-assessment results* **[2]**

Name of the Main Criteria	Average
1. Leadership	63
2. Strategy and policy	60
3. Human Resources Management	58
4. Partnerships and resources	71
5. Process and change management	62
6. Results of customer-oriented operation	69
7. Staff results (employee satisfaction)	57
8. Social impacts	71
9. Performance effectiveness	70
Organization average	**65**

Based on the self-assessment results, there are only two areas of the main criteria that perform less than the specified condition.

The CAF Self-Assessment Methodology Guide recommends that the report for management should only include key strengths and areas for improvement, due to easier clarity and facilitating management decision-making. Therefore, all the listed strengths and weaknesses in Chapter 3 were ranked to identify the key "strengths" and key areas for improvement listed below.

The defining strengths

Table 5. *The decisive strengths of the operation of HCC* [2]

1	It sets out official, professional values and rules of conduct to be followed, respecting the general values of the public sector.
2	It strengthens mutual trust, loyalty and respect between staff and managers.
3	It has developed an appropriate organizational structure.
4	The members of the HCC management team show a personal commitment and example to the quality of the official work and to the development of their own management activities.
5	The HCC maintains regular contact with partner organisations (NGOs, other public administrations and citizens) that are important for its operation.
6	It ensures transparency in its operations.
7	HCC ensures that all clients' cases are dealt with effectively, and that the case manager is identifiable; individual case management and consulting characterize the customer service activity, the administration is customer-friendly, service-type, flexible, receptive to individual situations
8	HCC ensures that its customers and partners have access to information that is important to them, which is otherwise public.
9	The physical accessibility of the HCC building is adequate.
10	It gives the main managers of each process adequate powers.
11	The HCC employs well-trained professionals, for whom it provides continuous training and the possibility of exchanging experiences (abroad).
12	The HCC representative regularly appears/voices in the local media in the field of social responsibility.

Key areas for improvement

Table 6. *Areas for improving the functioning of HCC* [2]

1	According to the reviews, there are many overburdened colleagues, there is an unequal division of labour. There is an effort to distribute tasks equally, but in practice this is not done in all areas. It would be necessary to assess workload and make informed and planned use of professional competences.
2	As part of effective internal communication, greater attention should be paid to the integration of new employees into the organization, e.g. in the case of hiring a new employee, to provide information about the organization and to familiarize them with the work of the partner areas.
3	According to reviews, the evaluation of the staff is often only formally implemented at the moment. It would be necessary to improve the methodology for objectives and evaluation, taking into account territorial differences and improving the material communication between managers and staff.
4	In addition to hearing the needs and initiatives of the employees, it is necessary to implement them and/or provide feedback to the staff about the measures taken or the reasons for their failure to do so.
5	It is necessary to systematically analyse its own organizational strengths and weaknesses, to this end it is advisable to carry out the CAF survey, self-evaluation regularly, evaluate and communicate the results.
6	By making even better use of the possibilities in the Task system, more attention should be paid to the parallel workload of employees when issuing strategic and operational tasks.
7	Staff and relevant external stakeholders should be involved in the process planning in all affected areas.

3.3. Further steps in self-evaluation

Considering that this was the first formally conducted CAF organizational self-assessment at HCC, it can be said that the self-assessment ended with a particularly good result. The evaluation has produced results that are suitable for identifying additional organisational development needs.

The review of the implementation of the development programmes and related action plans that can be determined by senior management based on the PDCA cycle will entail another CAF assessment. Monitoring progress is an ongoing task, the repetition of self-assessment is due within a year.

4. Conclusions

The results of the project were evaluated jointly under the leadership of Harghita County Council, and thus it was jointly established that CAF, as a professional tool, can be used effectively in the development of administrative activities in Romania, but it would be of great help in assessing performance if objectively recorded Romanian benchmark data and experience were available on the subject.

References

[1] *CAF 2013 Model – Methodological Guide to Organizational Self-Assessment.*
https://www.caf-network.eu

[2] Erdőssy I., Kerekes L.: *Report on the Strategic planning and performance management for citizens of Harghita County with the introduction of the CAF based quality management tool (CAFHR) project.* Miercurea Ciuc, 2021.

INTERPRETATION OF ROAD TRAFFIC NOISE CHANGES WITH NOISE MAPPING

Petra HAJNAL,[1] Dénes László KOCSIS[2]

University of Debrecen, Faculty of Engineering, Department of Environmental Engineering. Debrecen, Hungary

[1] *hajnalp0429@gmail.com*

[2] *kocsis.denes@eng.unideb.hu*

Abstract

With the advancement of technology and the drastic increase in the number of noise sources, environmental noise emission is increasing year by year. In the case of urban dwellers, noise from road traffic accounts for the largest share of noise pollution, with a number of negative health effects. The aim of our research is to monitor the road noise emission of the city of Debrecen in detail, using hourly traffic data. After data processing, various situations were modeled according to the MSZ 15036:2002 standard with the help of the IMMI noise mapping program. Overall, it can be said that the studies we have carried out support the high level and increasing trend of noise exposure.

Keywords: *traffic noise, noise exposure, noise mapping.*

1. Introduction

Noise pollution is a form of pollution that affects our daily lives, yet it is less talked about than other pollutants with a higher 'click-hunter value'. This is probably due to the fact that high noise is an inseparable part of the concept of big cities, so many people do not even think that continuous exposure can have negative health effects.

Noise maps usually provide only a state report of the city's yearly noise pollution. The aim of our research is to obtain a more detailed picture of how the rate of noise exposure varies in a given year, the extent to how the day and night noise emission values differ, and to examine the possible seasonal nature of the noise emission.

In the course of this study, we worked with a wide range of information, providing us with a suitable basis for detailed analysis.

2. Literature overview

2.1. Characteristics of road traffic noise

Traffic noise can arise from aviation; watercraft; train service and of course, cars. It includes not only the noise of the vehicle in motion, but the noise generated during the operation of the vehicle. The urban population is mainly exposed to noise from road traffic.

Road traffic noise is composed of a number of components, including engine noise; noise from tires and contact of the vehicle with the air. However, the noise pollution caused by vehicles is also closely linked to other conditions, such as the volume of traffic, the quality of the road surface, the number and proportion of heavy vehicles in traffic as well as the different topography, weather conditions, road conditions and other individual factors (e.g. intersections; and number of traffic lights) [1].

Problems arising from road noise pollution are constantly occurring in the vicinity of high-traffic road sections, so it is key to address them. In a previous publication, we analyzed the long-term changes in traffic noise through the examples of several road sections and concluded that a very significant increase in the traffic of passenger cars and light commercial vehicles can be observed in the case of the currently studied road

section and in general. We compared the 1995-1997 period average with the 2016-2019 period average [2]. According to the latest noise report 'Noise in Europe-2020' from the European Environment Agency (EEA), the growing trend will continue due to urban sprawl; and the increased demand for mobility [3].

2.2. Data of exposure

According to the interactive map of the *Noise Observation & Information Service for Europe*, 1,133,500 people in Budapest and 104,200 in Debrecen are exposed to high levels of road noise ($L_{den} \geq 55$ dB(A)) [4]. These data are of greater concern when compared to the total population of the cities: compared to the 2016 population data, about 64.6% of Budapest residents and more than half of the residents of Debrecen - 51.45 % -are affected.

The EEA states [5]: "In most European countries, more than 50% of the urban population is exposed to road noise levels of 55 dB or more during the day, in the evening and at night. According to the World Health Organization, this level of noise can already cause health problems. The European Union considers long-term exposure to noise levels above 55 decibels to be high noise levels."

The World Health Organization's (WHO) report 'Burden of disease from environmental noise' [6] which was published in 2011, looked at noise exposure in Western European countries, with data covering a 10-year period. It has been found that at least one million healthy life years are lost in Europe due to noise emissions, and while other forms of pollution are becoming less and less present in the environment; noise exposure is increasing.

Research suggests that among people living on noisy road sections, exposure to noise can cause temporary; or even chronic physiological process changes. This influence, as well as the noise exposure, can be permanent and can lead to major problems such as high blood pressure and consequent heart disease, as well as an increase in hearing threshold [7].

3. Methods

3.1. Area of analysis

The road section with code number 1039 has been designated as the study area, which marks the section of the main road 4 between *Sámsoni út* and *Faraktár utca* in Debrecen. Within the 1039 section, the focus was on the *Kassai út* road sec-

tion and its immediate surroundings. The traffic passing here can be considered high in terms of the city, each vehicle category appears on the section to a significant extent, so the road section is a valid representation of the other roads in the city with similar characteristics.

A noise map was prepared to examine the surroundings of the 'Kassai út' road section. The buildings in the vicinity of the area were also modeled on the noise map, so the noise-reflecting effects of each building can be examined. In real life, people are affected not only by the noise load from a road section, but also by the noise emission emitted by the total traffic in the given area, but in the case of the study area, the dominance of the Kassai road is clear.

3.2. Traffic data

3.2.1. Acoustic vehicle categories

It is essential for noise assessment methods to classify different types of vehicles into acoustic vehicle categories, as the higher presence of each category on the roads significantly influences the amount of noise load emitted by the road. Traffic data can only be interpreted after classification into acoustic vehicle categories. Class classifications are based on the 93/2007. (XII. 18) KvVM regulation, the following can be read in it: Passenger cars and vans belong to category I; motorcycles and mopeds ; solo buses and light goods vehicles (up to a total weight of 7000 kg) fall into the II. category, III. category includes articulated buses, solo heavy goods vehicles and lorry combinations.[8]

Contrary to Hungarian legislation, the CNOSSOS-EU noise assessment method, created thanks to the European Union's legal harmonization efforts, currently has 5 main categories, which differs from the Hungarian one in that motorcycles and mopeds are in category 4, and there is also a 5., open category to meet future needs [1].

3.2.2. Average Daily Traffic

A record, named 'Az országos közutak XY. évre vonatkozó keresztmetszeti forgalma' can be downloaded from the website of Magyar Közút Nonprofit Zrt. The document contains values for the annual average daily turnover (acronym in Hungarian: ÁNF), which is essential for calculating the so-called $L_{AM,kö}$, values. In order to access the ÁNF data, the cross-sectional traffic data is given a specific code number based on the traffic road category, the location of the road according to the county, the number of the examined sec-

tion and the boundary sections of the examined section.

The aim of the current research was to monitor the distribution of the noise load as a function of the change in traffic, therefore the document issued annually by Magyar Közút Zrt. does not provide us with a sufficiently detailed picture. The amount of information in the report is not sufficient for research purposes because, as its title suggests, it only includes traffic data for each cross-section for the annual situation. We obtained access to the detailed, hourly traffic data after contacting Magyar Közút Zrt.

3.2.3. Hourly traffic data

Detailed hourly traffic data for four years (2015, 2016, 2017, 2019) were available to us. The traffic count on the examined section was performed by a Miniloop measuring instrument in intermittent operation. The tool could only measure the number of vehicles passing through two lanes. For the years under study, the passing vehicle numbers provided by the instrument, registered by the two loops, were given in month/day/hour format. The raw traffic count data sent by Magyar Közút Zrt. were systematized and divided into acoustic categories in order to produce the detailed traffic data required for the noise maps.

3.3. IMMI noise mapping programe

We used one of the market-leading noise mapping programs, IMMI, for noise mapping. The program of German origin offers many possibilities in different areas of noise mapping. During the examination, the program performed a noise calculation based on the entered traffic data (in accordance with the valid Hungarian legislations and the current regulations of CNOSSOS-EU).

The noise load data of the examined road section can be entered into the system in 3 different ways: with hourly distribution data; in the case of outdoor measurements, the ÁNF for the year and the hourly traffic data recorded during the measurement period, and the pre-calculated sound pressure level values can also be entered into the program. Traffic data is always provided for each acoustic vehicle category. In our case, the hourly distribution data proved to be the most suitable for processing the results of the data analysis.

In the basic map, Kassai út is marked as a line source, the buildings close to the measurement point were modeled one by one according to the Debrecen town plan (based on satellite images, we can input more details, such as buildings

Figure 1. *Modelled image of the test area*

height), the more distant blocks of buildings were depicted as residential areas. In order to be able to examine how the noise emission values acted at a point, we added a measuring point under the number 16 on Kassai út, which is shown on the map with a microphone icon. At this point, we had previously performed road noise measurements in several cases..

4. Results

4.1. Data processing of the hourly traffic

The trafficmeter provides hourly data for the observed area, so daytime and nighttime traffic can be determined, which is advantageous, because the 27/2008. (XII. 3.) KvVM-EüM joint decree sets separate limit values for the day (06-22 hours) and night (22-06 hours) assessment period. According to the law, in the case of motorways and main roads belonging to the national road network, the amount of LAM, 'kö in residential areas built in large cities may not exceed 65-; and 55 decibels at night.

It was crucial to classify the data into acoustic vehicle categories, which were based on the annual reports issued by Magyar Közút Kft. In the examined years, the distribution data were analyzed, and then the traffic volume data belonging to each class were compared with the total number of vehicles passing through the year, after that the total traffic numbers were divided by the number of persons in each class. Thus, the following ratios were obtained as a result:

Table 1. *Calculated ratios for acoustic vehicle categories*

Acoustic vehicle category	Ratio
I.	0.914
II.	0.0396
III.	0.0462

The hourly vehicle turnover data for the two lanes were summed and then aggregated for the given time of day (day and night). In addition, we determined the total monthly turnover, the monthly average turnover, the minimum - maximum hourly turnover of the given month and the standard deviation of these values. These evaluations were performed for each year examined and then summarized annually for that month. After scaling, the following turnover data were obtained for the examined years, daytime and evening time (In **Table 2** the notation 'D' and 'N' after the examined years refer to the daytime and nighttime assessment periods, respectively):

Table 2. *Average hourly distribution data per day (D: day, N: night) for the studied years by acoustic vehicle categories (unit: vehicle / hour)*

	I. cat.	II. cat.	III. cat.
2015D	877.59	38.02	44.39
2015N	156.83	6.79	7.93
2016D	907.82	39.33	45.92
2016N	162.72	7.05	8.23
2017D	867.19	37.57	43.86
2017N	218.28	9.46	11.04
2019D	1068.14	46.27	54.03
2019N	163.49	7.08	8.27

The information obtained during the data analysis made suitable for processing by the IMMI noise mapping program.

4.2. Noise mapping of the studied years based on the processed traffic data

The noise mapping program is multinational; it also includes the CNOSSOS-EU noise assessment method, which has been developed as a result of EU harmonisation.. The noise mapping was carried out in accordance with standard MSZ 15036: 2002 and was also performed on the basis of CNOSSOS-EU, but it is important to emphasize that the European method is still an adaptation therefore these values may differ in the future.

For the four years studied, the data were entered into the program, so the sound power values L_w or the road section were determined.

Based on **Table 3** it can be stated that the level of noise exposure during the years is similar, but both for daytime; both night values are high.

The highest noise emissions affect residents and passers-by directly along the roads. Moving away from the line source, the amount of noise emis-

Table 3. *Sound power level values of the examined years*

Year/L_w' (dB(A))		MSZ	CNOSSOS
2015	Day	82.23	80.6
	Night	75.15	73.1
2016	Day	82.36	80.7
	Night	75.33	73.2
2017	Day	82.19	80.5
	Night	76.59	74.5
2019	Day	82.95	81.4
	Night	75.35	73.3

Figure 2. *Daytime noise map for 2015 (from hourly daily averages, according to MSZ 15036: 2002)*

sion caused by one road section becomes smaller and smaller, the more distant area is no longer affected, the effect of the locally closer line sources must be taken into account.

Noise maps were prepared to examine the annual noise propagation properties, however, due to space limitations, only one map is included in the publication (**Figure 2.**) .

4.3. Processing minimum-maximum traffic data

Hourly traffic data has helped us to examine the extent to which noise exposure may deviate within a year. The highest yearly values, and the lowest traffic days were used as the basis for the analysis.

We recorded a noise load point on the map at the 16th location of Kassai út, which used to be a measuring point, so it became possible to determine whether the limit value is exceeded on the minimum and maximum traffic days for the given year and what the difference is.

According to the Hungarian legislation, the measuring point was marked on the map 2 meters in front of the façade, at an assessment height
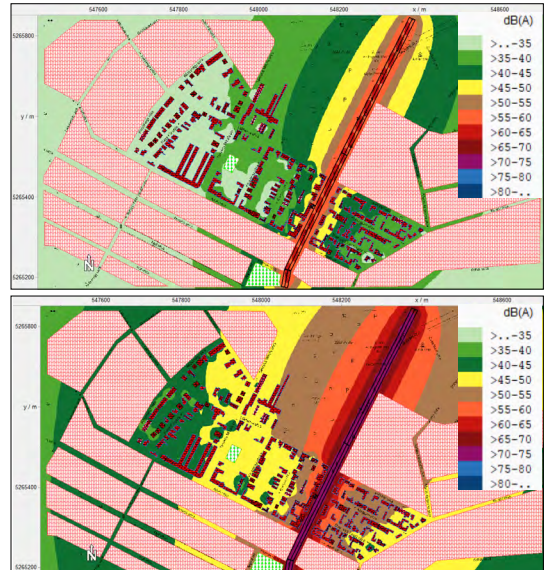
of 1.5 meters. The results of the sound power level examined on the basis of the minimum-maximum traffic volumes of the obtained years show a large difference. It is worth noting that the L_{Aeq} sound pressure levels for the night always exceeded the 55 dB (A) limit, even at the minimum values.

Of the four years, 2019 has the absolute minimum-maximum value; on the least busiest day, 2306 vehicles passed, while on the busiest day, 27391 vehicles passed section 1039. There is a big difference in the amount of noise emitted by vehicles passing through the road section: 72.8 dB (A) during the minimum day and 62.3 dB (A) at night, and the maximum turnover day. 84.1 dB (A) daytime and 76.6 dB (A) nighttime sound power levels were observed. The difference between the two daytime releases is particularly large; the difference is 11.3 decibels. The contrast between the two values is well illustrated by images of **Figure 3**.

Table 4. *Minimum-maximum traffic day for a given year*

Minimum-maximum traffic day for a given year (vehicle/day)	2015	Date	04.21.
		MIN	4238
		Date	06.05.
		MAX	22252
	2016	Date	04.13.
		MIN	2872
		Date	06.10.
		MAX	23724
	2017	Date	09.14.
		MIN	5048
		Date	12.22.
		MAX	24606
	2019	Date	09.18.
		MIN	2306
		Date	09.13.
		MAX	27391

Table 5. *L_{Aeq} sound pressure levels at minimum - maximum days [dB(A)]*

	Day	**Night**
2015 MIN	62.49	56.55
2015 MAX	69.27	61.95
2016 MIN	60.36	57.39
2016 MAX	68.96	66.18
2017 MIN	63.05	58.52
2017 MAX	69.57	63.35
2019 MIN	58.79	58.29
2019 MAX	70.09	62.51
Limit value	**65 dB(A)**	**55 dB(A)**

Figure 3. *Noise map of the absolute minimum and maximum traffic days of the examined years*

4.4. Analysis of periodic properties of noise emission

The traffic volume for the winter and summer months of the studied years was also modeled, the main purpose of which was to examine the possible seasonal characteristics of noise emission.

There is no significant difference between the daytime values for January and August but in the night-time load data, there is a bigger difference observed for the summer months. (**Table 6.**) This increased traffic in the summer months is the reason for higher levels of night noise exposure.

4.5. Number of people affected by noise exposure from the road section

The IMMI noise mapping program can be used for various parameters; so-called thematic maps can also be produced. One of these thematic maps also shows the number of people living in certain

Table 6. *Sound power level values for January and August [dB(A)]*

$L_{w'}$ [dB(A)]		January	August
2015	Day	82.16	82.44
	Night	73.53	75.31
2016	Day	81.87	82.69
	Night	73.49	75.51
2017	Day	81.58	82.65
	Night	73.48	75.12
2019	Day	82.46	83.04
	Night	74.23	75.93

residential buildings, which is determined by the IMMI program based on the parameters of the residential buildings. Based on this map, it can be examined the number of people directly affected by the noise load caused by the given road section can be determined.

The software can also run detailed calculations on the topic of involvement; so it can determine how many people are actually affected by noise exposure ranges at a certain distance from the source. In the immediate vicinity of the studied section, approximately 1059 inhabitants in our modeled area - based on the analysis of the program - are involved in the noise load from section 1039.

Most residents are in the 45-50 decibel range, with about 343 people in this category. The maximum load range is 65-70 dB, affecting 24 people. It is worth noting that more people fall into smaller load classes because there are condominiums that can accommodate more residents away from the road section than in the immediate vicinity of the road section.

5. Conclusions

We examined the noise load in the vicinity of the road section that is the subject of our study between 2015 and 2019 based on traffic data from the road operator. In addition to the annual average traffic data, we also produced noise maps for the lowest and highest traffic days using the current Hungarian standard and CNOSSOS-EU. At a set point, we examined compliance with the limit values for road noise. Based on this, we have revealed that the limit value is exceeded even during the lowest traffic days of the year. Comparing the January and August averages, we identified a significant increase in nocturnal noise emission for the summer values of the road section.

As a result of our investigations, we obtained a detailed picture of the development of noise load in the case of a high-traffic, urban road section, determining the daily noise characteristics for each day.
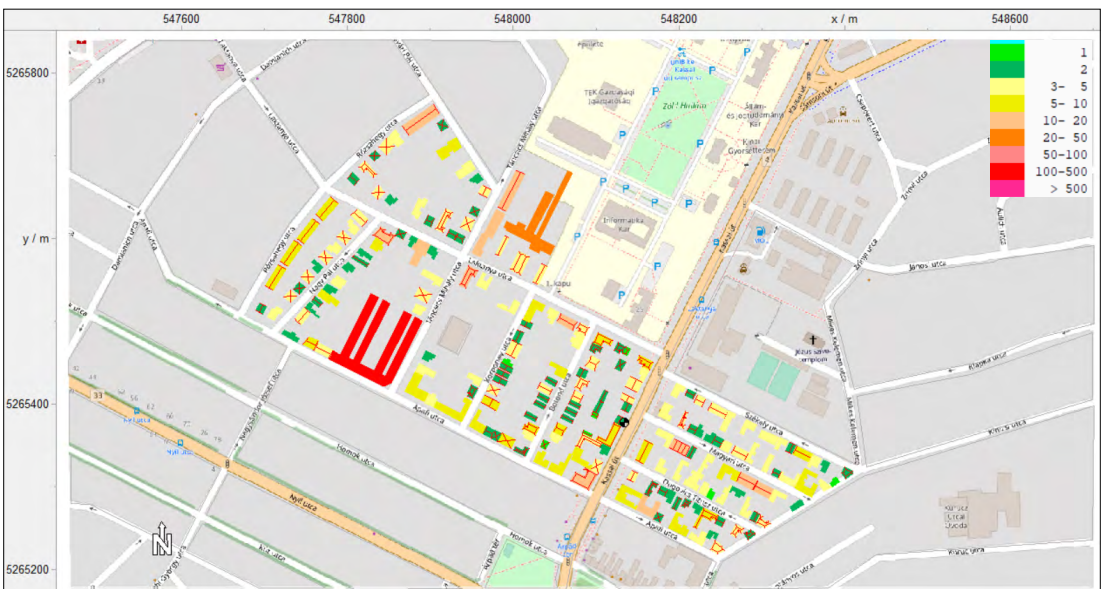
Figure 4. *Population of the immediate environment of section 1039 [persons]*

References

[1] Commission Directive (EU) 2015/996 of 19 May 2015 establishing common noise assessment methods according to Directive 2002/49/EC of the European Parliament and of the Council.

[2] Kocsis D., Hajnal P.: *Long-term Road Traffic Noise Changes in an Urban Area.* In: ICSV27 Proceedings. Prága, Czekoslovakie. 2021. 5.

[3] European Environment Agency: Environmental Noise in Europe-2020, no. 22/2019, 2020. 47.

[4] EEA, Noise Observation & Infromation Service for Europe, EU. accessed; 2021.10.08)

https://noise.eea.europa.eu (

[5] EEA, Number of Europeans Exposed to Harmful Noise Pollution, EU. 2020. Number of Europeans Exposed to Harmful Noise Pollution Expected to Increase — European Environment Agency (europa.eu) (letöltés ideje: 2021. 10. 08)

[6] WHO: Burden of Disease from Environmental Noise, 2011. 237.o.

[7] Koren E.: *Környezettan.* Széchenyi István Főiskola, Győr, 1995. 107.

[8] 93/2007. (XII. 18.) KvVM statue
https://njt.hu/jogszabaly/2007-93-20-0N

ABOUT THE GRINDING OF GEAR HOB'S RAKE FACE

Norbert HODGYAI,[1] Mircea Viorel DRĂGOI,[2] Ferenc TOLVALY-ROȘCA,[3] Márton MÁTÉ[4]

[1] „Transilvania" University of Brașov, Doctoral School, Brașov, Romania, hodgyai@ms.sapientia.ro

[2] „Transilvania" University of Brasov, Faculty of Manufacturing engineering and Production Management, Brașov, Romania, dragoi.m@unitbv.ro

[3] Sapientia Hungarian University of Transylvania, Faculty of Technical and Human Sciences, Department of Mechanical Engineering, Tîrgu-Mureș, Romania, tferi@ms.sapentia.ro

[4] Sapientia Hungarian University of Transylvania, Faculty of Technical and Human Sciences, Department of Mechanical Engineering, Tîrgu-Mureș, Romania, mmate@ms.spientia.ro

Abstract

The most simple and robust construction of the monolithic gear hobs present a common helical rake face for a given line of teeth, whose generatrix is a straight-line segment perpendicular to the hob's axis while its directory is a helix, perpendicular to the pitch helix. As a consequence, constructive rake angles are zero on all edges. Total curvatures of such a surface are negative. Thus, it can be grinded only using the conical surface of a platter type grinding wheel, or a grinding bit. Despite this, some industry practices, possibly for reasons of simplicity and cost lowering, involve the plain grinding surface, supposed to a helical motion. This paper deals with the CAD-simulation of the grinding process using the plain wheel surface, and it shows the differences between the theoretical and rake face and the real obtained helical surface.

Keywords: gear-hob, rake face, grinding, meshing, through-cut.

Notations

m_n – normal module [mm];
α_0 – normal rack profile angle [°];
p_C – rake helix parameter [mm];
R_0 – pitch radius, [mm];
R_a – addendum cylinder radius, [mm];
R_f – dedendum cylinder radius [mm];

λ_0 – leading helix declination angle of the gear-hob [°];
λ_x – crossing angle between the axis of the gear hob and the plane face of the grinding wheel, [°];
a_w – axis distance [mm];
v – surface normal unit vector

1. The mathematical model of the rake face

A gear hob's rake face usually is a helical surface of parameter p_C **[1, 2]**, meshed by a straight line that crosses the gear hob's axis (**Figure 1**). Thus, the parametric equations of the helix surface denoted with Σ are as follows:

$$\begin{cases} x_2(u,\varphi) = p_C\varphi \\ y_2(u,\varphi) = u\cos\varphi \\ z_2(u,\varphi) = -u\sin\varphi \end{cases} \tag{1}$$
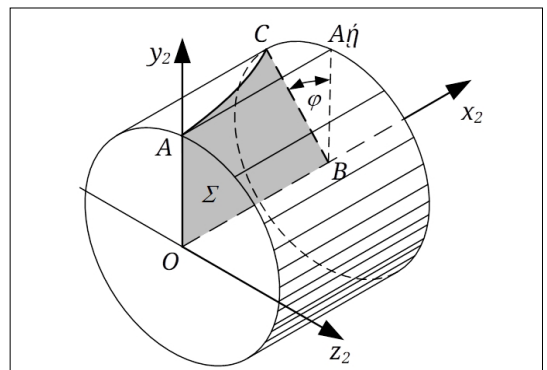

Figure 1. AThe theoretical helical rake face

2. The relative motion between the grinding wheel and the gear hob

Let us consider the geometric elements shown in **Figure 2.** Three frames will be used here: S_0 is the fixed frame, while S_1 and S_2 are connected to the grinding wheel, and the gear-hob. The relative motion of the grinding wheel related to the gear hob results from a rotation of angle φ sof the gear- hob about its own axis while the grinding wheel is translated, corresponding to this, along the same axis with a distance of $p_c\,\varphi$ corresponding to the parameter of the leading helix. Mathematically, this can be formulated using the matrix equation below:

$$\underline{r}_2 = M_{20}\,M_{01}\underline{r}_1 \tag{2}$$

The expressions of the matrices in eq. (2) are the followings:

$$M_{20} = \begin{pmatrix} 1 & 0 & 0 & 0 \\ 0 & \cos\varphi & \sin\varphi & 0 \\ 0 & -\sin\varphi & \cos\varphi & 0 \\ 0 & 0 & 0 & 1 \end{pmatrix}$$

$$M_{01} = \begin{pmatrix} \cos\lambda_x & 0 & \sin\lambda_x & p_c\varphi \\ 0 & 1 & 0 & a_w \\ -\sin\lambda_x & 0 & \cos\lambda_x & 0 \\ 0 & 0 & 0 & 1 \end{pmatrix} \tag{3}$$
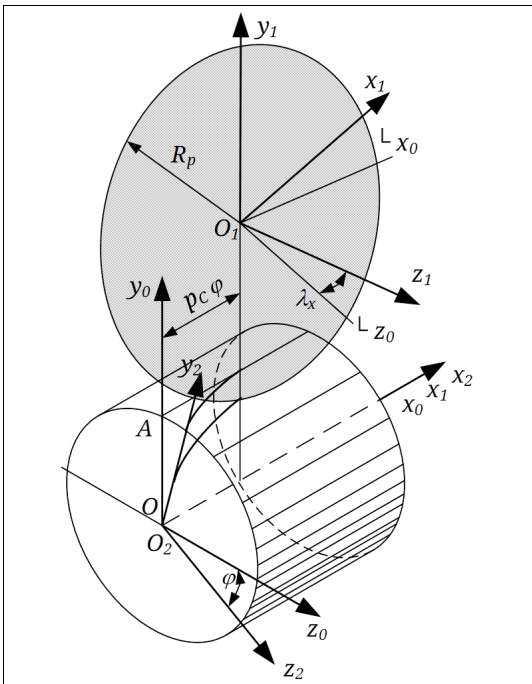

Figure 2. *Ahe applied frames*

The axis distance results from the sum of dedendum radius of the gear-hob and the largest radius of the grinding wheel:

$$a_w = R_f + R_p \tag{4}$$

The equation of the plane surface of the grinding wheel is given below in polar coordinates:

$$\begin{cases} x_1(\rho,\theta) = \rho\sin\theta \\ y_1(\rho,\theta) = -\rho\cos\theta \\ z_1 = 0 \end{cases} \tag{5}$$

With the use of eq. (2), it is possible to obtain the motion of any point of the grinding wheel related to the gear hob. Thus, an estimation of the shape of the resulting flute part – the rake face – can be achieved.

First of all, it must be stated here that the grinded rake face results here not from meshing, but from a continuous and infinite series of through-cuts. The through -cut is a specific case of generating, when the tool's imprints are not tangent to the resulting surface, but they intersect it. No common normal vector can be defined here – at least inside the limits of the machined part. A study of the phenomenon related before can be performed using the so called Monge-brick [3].

Let's consider the helix surface given by eq. (1). Omitting the detailed computing [4] the invariant quantities of the first and the second fundamental form are as follows:

$$\begin{cases} E = \dfrac{\partial r}{\partial u}\cdot\dfrac{\partial r}{\partial u} = 1 & (6) \\[2mm] F = \dfrac{\partial r}{\partial u}\cdot\dfrac{\partial r}{\partial \varphi} = 0 \\[2mm] G = \dfrac{\partial r}{\partial \varphi}\cdot\dfrac{\partial r}{\partial \varphi} = p_c^2 + u^2 \\[2mm] L = -\dfrac{\partial r}{\partial u}\cdot\dfrac{\partial v}{\partial u} = 0 \\[2mm] M = -\dfrac{1}{2}\left(\dfrac{\partial r}{\partial u}\cdot\dfrac{\partial v}{\partial \varphi} + \dfrac{\partial r}{\partial \varphi}\cdot\dfrac{\partial v}{\partial u}\right) = \dfrac{p_c}{\sqrt{p_c^2 + u^2}} \\[2mm] N = -\dfrac{\partial r}{\partial \varphi}\cdot\dfrac{\partial v}{\partial \varphi} = 0 \end{cases}$$

The principal curvature's algebraic equation of second degree *(EG − F²) k² −(EN − 2FM + GL) k + (LN − M²) = 0* [4] becomes here:

$$(p_c^2 + u^2)k^2 - \dfrac{p_c^2}{p_c^2 + u^2} = 0 \tag{7}$$

whose roots are:

$$k_{1,2} = \pm\dfrac{p_c}{p_c^2 + u^2} \tag{8}$$

Either interpreting expression (8) or analyzing the sign of $LN−M^2$ it results that every point of the surface is a hyperbolic point, thus the total or Gauss curvature is negative. From here it results that the tangent plane (i.e., perpendicular to the normal vector in the considered point) intersects the surface in any point along it, due to the fact that the normal curves corresponding to the main curvatures are located on opposite sides of this plane. In conclusion, the surface given by eq. (1) is impossible to grind using a flat grinding wheel. However, practice shows that grinding using a flat surface can lead to a continuous smooth surface, although the modeling of this cannot be realized by applying the meshing theory.

The statement above was verified by a numerical simulation, performed on a gear-hob of $m_n = 5\,\text{mm}$, $\lambda_0 = 3,5°$ and one thread. The point-clouds generated by the flat side of the grinding wheel were realized for the axis cross angle values of $\lambda_x = \lambda_f$, $\lambda_x = \lambda_0$ and $\lambda_x = \lambda_a$. **Figures 3** and **4** show the point-clouds resulting for the smallest and the largest crossing angle value. Here, it must be emphasized that the larger the crossing angle λ_x the greater the resulting difference between the theoretical surface and the point-cloud.

In any case the point-cloud covers the ideal surface, namely the ideal surface points are situated inside the border of the generated point-cloud. Consequently, the grinding operation produces continuous through-cuts or interferences.

In the following, real grinded surfaces will be studied using CAD models.

3. The structure of the CAD-model

Construction of an efficient CAD-model requires consistent knowledge of the determining geometric elements of the gear-hob **[5]**. Here must be taken into consideration the technical solutions mentioned in the literature, together with the peculiarities of manufacturing using classical machine-tools and thus the effects of the technological simplifications.

3.1. Peculiarities of gear-hob manufacturing

Involute worm gear transmission is that particular case of helical involute gear pairs, where the inclination angle of the tooth of one of the elements becomes so large that the tooth becomes a thread and thus the gear turns into a worm.

The traditional involute gear hob derives from an involute worm. Intersecting this with a finite number of equidistant flutes results in the teeth-
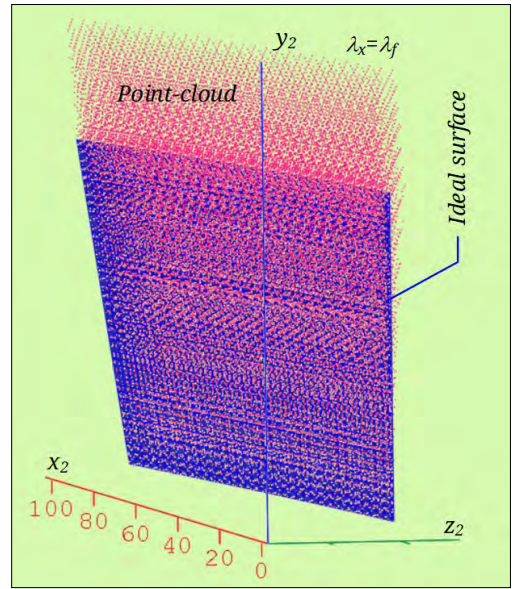

Figure 3. *The trace of the grinding wheel (pink) and the ideal surface (blue) for the smallest axis crossing angl $\lambda_x = \lambda_f$.*
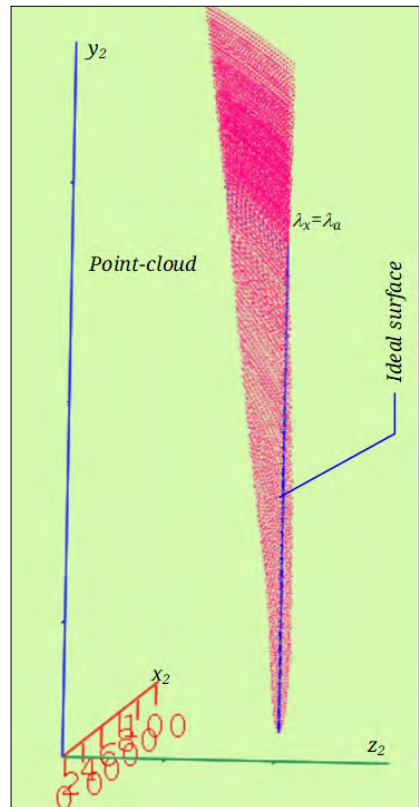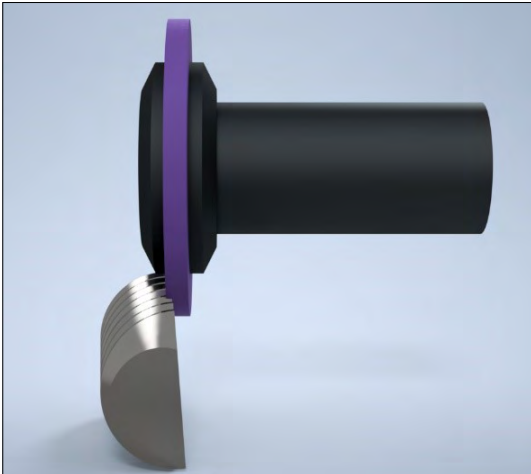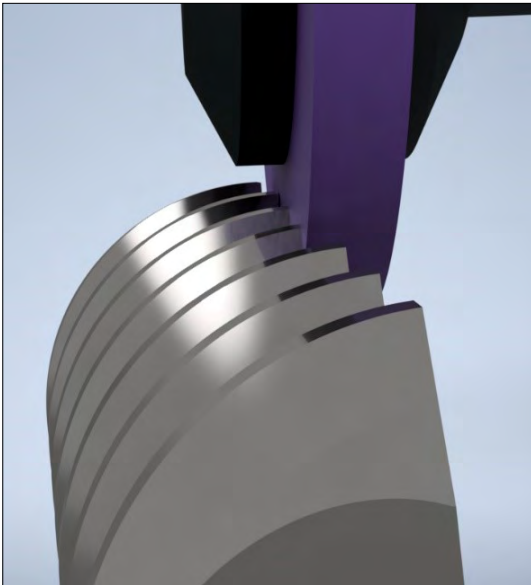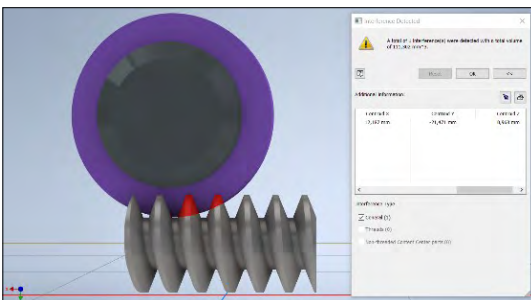

Figure 4. *The trace of the grinding wheel (pink) and the ideal surface (blue) for the largest axis crossing angle $\lambda_x = \lambda_a$.*
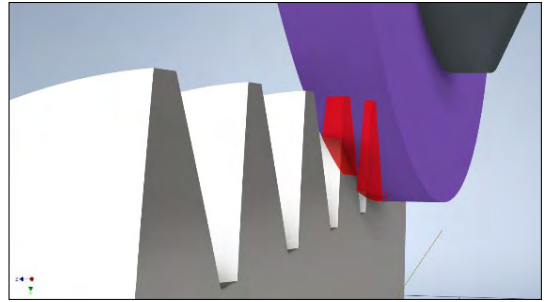
Figure 5. *The model of the rake face and the grinding wheel*

Figure 6. *The through-cut of the grinding wheel*

Figure 7. *Analysis of interference*

Figure 8. *The interference in 3D representation*

lines that later become subject of the relieving operation in order to realize the relief angles on all cutting edges. A remarkable property of the helical rake face consists in its perpendicularity on the leading (pitch) helix of the worm. Therefore, the constructive rake angle result is 0o.

When machining a gear-hob on classical machine-tools, certain simplifications were implemented. Due to the fact that the axial section the flank line of the involute worm is curved, it was in practice replaced often by a straight normal profiled ZN1-type worm **[6]**.

The relevance of the helical rake face consists in producing approximatively equal constructive geometry on the lateral edges, in order to equalize the durability of edges on both tooth flanks.

The CAD-model was created for the sharpening of the rake face with the flat side of the grinding wheel. Different axis crossing angles and wheel diameter values were considered. .

4. Numerical evaluation

As a consequence of the interference phenomenon presented above the resulting rake face is truncated. The error value depends on the grinding wheel diameter and the axis crossing angle.

4.1. The influence of the axis crossing angle

The influence of the axis crossing angle (**Figure 9**) was investigated for three distinct values that equal respectively the dedendum, the pitch and the addendum helix angle.

The results are shown in **Table 1.** Numerical values indicate the maximum of interference, considered in the normal direction.

4.2. The influence of wheel diameter

The diameter of the grinding wheel also influences significantly the value of the interference. The obtained results are also included in **Table 1.** The considered diameters were respectively 112.5 mm, 160 mm and 200 mm.
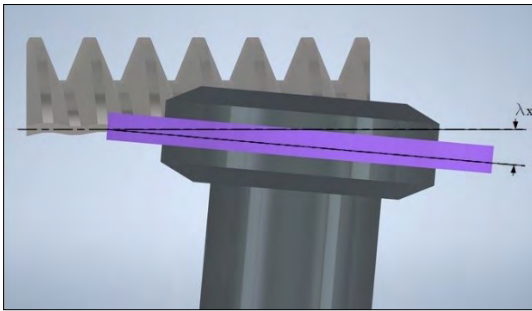
Figure 9. *The representation of the axis crossing angle (lx)*

Table 1. *Interference values for different crossing angle and diameter values.*

Maximal normal interference [mm]				
No.	Wheel diameter [mm]	la	lo	lf
1	112.5	1.136	0.965	0.792
2	160	1.268	1.082	0.893
3	200	1.511	1.291	1.064

5. Conclusions

Gear-hob sharpening with a disk type grinding wheel is a common manufacturing technology. There exist a lot of demonstrative videos on the subject. The setup of a flat disk is simpler than those of a profiled grinding wheel. The disadvantage of the procedure arises from the interference that is inevitable. In the real process, errors of interference cumulate with the grinding machine setup errors and grinding wheel errors.

All these errors will result in inappropriate functional edge geometry and profile errors. As a result, a decrease in durability and precision of the manufactured gear will occur.

References

[1] Máté M.: *Hengeres fogaskerekek gyártószerszámai.* Erdélyi Múzeum-Egyesület, 2016.
https://doi.org/10.36242/mtf-12

[2] Radzevich S. P.: *Gear Cutting Tools: Fundamentals of Design and Computation.* CRC Press, NY, 2010.

[3] Balajti Zs., Dudás I.: *The Monge Theorem and Its Application in Engineering Practice.* International Journal of Advanced Manufacturing Technology, 91/1–4. (2017) 739–749.
https://doi.org/10.1007/s00170-016-9763-1

[4] Atanasiu Gh.: *Algebra liniară, geometrie analitică și diferențială, ecuații diferențiale.* All, Bucureşti, 1998.

[5] Tolvaly-Roşca F.: *A számítógépes tervezés alapjai. AutoLisp és Autodesk Inventor alapismeretek.* Erdélyi Múzem Egyesület, 2009.
https://doi.org/10.36242/mtf-07

[6] Hollanda D.: *Aşchiere şi scule.* Reprografia I.I.S. Tg. Mures, 1982.

[7] Hodgyai N., Máté M., Tolvaly-Roşca F., Drăgoi M. V.: *Peculiarities of the Grinding Process of a Gear Hob Helical Rake Face.* Acta Universitatis Sapientiae, Electrical and Mechanical Engineering, 13. (2021) 39–51.
https://doi.org/10.2478/auseme-2021-0004.

IMPACT ENERGY ABSORBTION BY ACTIVE BRAKING

József KERTÉSZ,[1] Tünde Anna KOVÁCS[2]

[1] Obuda University, Doctoral School on Safety and Security, Budapest, Hungary;
University of Debrecen Faculty of Engineering, Air- and Road Vehicles Department, Debrecen, Hungary,
kertesz.jozsef@eng.unideb.hu

[2] Obuda University, Bánki Donát Mechanical and Safety Engineering, Budapest, Hungary,
kovacs.tunde@bgk.uni-obuda.hu

Abstract

Due to urbanization and the significantly increasing number of vehicles, urban roads are becoming more congested day by day, with the result that the rear-end collision has become the third most common type of collision. By developing and integrating active and passive safety systems, car manufacturers are working to prevent accidents and reduce the consequences of an accident. The present study examines a braking procedure and its applicability based on the integration of a passive and active safety system and provides development guidelines for the reduction of personal injuries and property damage in the event of a rear-end accident.

Keywords: impact energy, brake assistant, rear-end collision, absorption.

1. Introduction

Owing to the significant development of sensors and control systems, car manufacturers have more and more possibilities to enhance the safety system of vehicles. The sensor-based controlling system which is designed to avoid accidents, can be called an active safety system. In a vehicle, passenger body integrity is provided by the passive safety system. All passive safety systems are responsible for the physical safety of motor vehicle occupants in the event of an accident [1] The development of vehicle safety systems has reached astonishing proportions, as vehicle transport, which has met the need for mobility most widely, has been accompanied by the need for safety from an early age. [2] Although the technologies used today are suited to meet the requirements of transport safety, due to the remarkable increase in the number of vehicles on our roads, accidents numbers are increasing in number day-by-day. Therefore the development of the vehicle safety system is still a very important issue in the vehicle industry. Qualitative and quantitative improvement within the vehicle industry always involves the need for safety. In the case of vehicle

safety improvement, it is not only the present requirements that must be considered, but also the demands of the future, such as autonomous transport. Safety and autonomous transport are closely related concepts, since by applying them, inattentive and irresponsible human behaviour–based accidents will be mostly avoided, or reduced. [3] Considering the expansion of autonomous transport, although active safety system fields will be developed, the necessity of the passive safety system cannot be ignored. This study introduces an active and passive element combined integrated safety system, and it deals with the development and application possibilities of this system, focusing on rear-end collision problems.

2. The circumstances of the accidents

According to the NHTSA (National Highway Traffic Safety Administration) report, 30% of road accidents are the result of rear-end collisions, which means the third most common collision types are side and frontal accidents.[4] 80% of these accidents are triggered by the following situations: [5]
– collisions in longitudinal traffic;
– collisions in a traffic jam;

– collisions with a vehicle that is stationary at a traffic light;
– collisions with a vehicle that is just about to turn left.

The statistics of the impact overlap is very important information in researching improvement in the effects of rear-end collisions. In respect of impact research, the overlap can be considered as the distance of the longitudinal axis of the vehicles expressed in per cent form. **Figure 1** shows an explanation of this overlap.
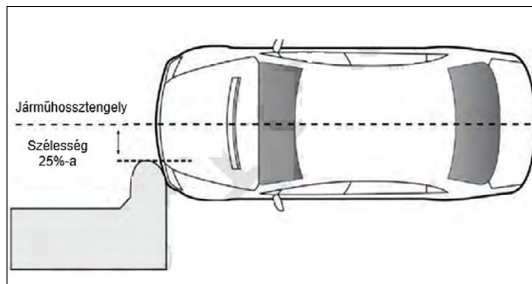
Knowledge of the statistical occurrence of the overlap value is important during the development, as it is possible to develop the active and passive safety systems optimally. Consideration of the previously listed traffic situations and recent investigations confirms that 90% of the rear-end collision are an overlap type accident, so the distance of the axis is low or almost zero. **[5]** A The incidence statistics of rear-end collision overlap can be expressed with a Gauss diagram, where the maximum of the chart indicates the minimum overlap values frequency. (**Figure 2**)
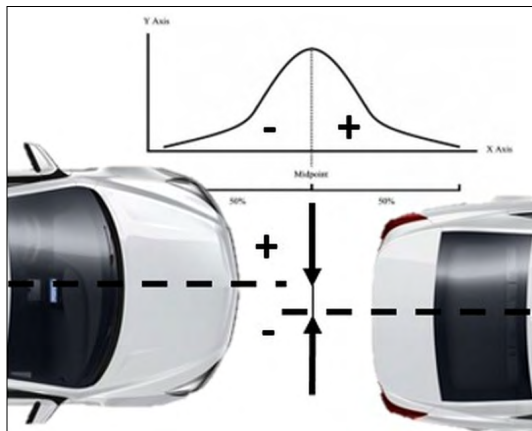
The effect of rear-end collisions is influenced by the difference in the kinematic energy of each participant vehicle, so the mass and velocity of the vehicles must be known. Accordingly, rear accidents can be divided into two groups. The first can be classified as where both participants are in motion. The other typical impact type is where the velocity of the frontal participant is zero, or almost zero.

3. Dilemma of the active and passive safety system

The ESP (Electronic Stability Program), the Active Brake Assistant and the ACC (Adaptive Cruise Control) active safety systems are working in synergy cooperation to avoid the rear-end collision. Collision is avoided by autonomous braking of the vehicle coming from behind so that these systems intervene by overriding the driver for safety reasons. Thanks to this reflex-based safety system, a remarkable proportion of the rear accidents can be avoided, or the impact energy can be reduced significantly. In the case of impact, the real consequences of these accidents are not only influenced by the reflex-based system of the rear vehicle but the frontal (frequently innocent) vehicle's safety system also. This context can be expressed by the Haddon matrix. (**Figure 3**) According to this the final outcome of the accident is not only influenced by the pre- but the actual- and the post-pa-

Figure 1. *Explanation of overlap* **[6]**

Figure 2. *Frequency of overlap.*

Figure 3. *Haddon-matrix.*

rameters of the car, driver and environment. This means that from the moment of the impact the passive safety system of the participants plays a notable role in the effects of the collision.

This system aims to prepare the innocent frontal vehicle for the accident before the moment of impact, and actuate the necessary safety system for the safety of the passengers. However, unfortu-

nately, the previously listed sensor-based systems integration is not enough to prepare the vehicle itself for the impact. **Figure 4** also confirms, very frequently the accidents, where the frontal participant is stationary, so the ESP can not provide information.

The vehicle coming from behind can not be detected by the ACC detector, since that is mounted on the front of the vehicle, and it has sensing angle limitations. The blind spot detector which is mounted behind the rear bummer shell is not suited for reliable detection of the fact and the velocity of the objects arriving from the back. Therefore, the optimization of the safety system to reduce the consequences of a rear-end accident always requires the installation of an additional radar integrated into the rear bumper. The installation position of the radar is helped by the statistics of the overlap, according to which the middle longitudinal axis of the vehicle is the most optimal position for the sensor.

4. Limitation of the radar

The installation position is supported by the overlap statistics, however, it mustn't be neglected that the radar has operational and reliability limitations. The reliability of the radar's detection of different materials and shaped objects must be taken into consideration. The reliability of the system when considering the weather can not be guaranteed however; snow and ice on the bumper can cover the sensing surface of the sensor. An important aspect is also the precise calibration of the radar sensitivity and the range. Radar calibrating for short-range can reduce the number of unnecessary alarms, nevertheless, there would not be enough time to prepare the vehicle for the impact. The over-calibrated radar would give a frequent unnecessary alarm for the driver, and it would be actuated also when it is not justified. Intersections and the junctions have also an important role in terms of the calibration since false detection of the situations gives a needless alarm (**Figure 5**). The frequent alarm results in inconvenience for the driver, and no sympathy for the system. The previously mentioned shape recognition could also have reliability problems. Namely, sometimes the size of the subject approaching from behind frequently does not corresponding with its real mass. Let's think of a truck, the radar can recognize and handle the size of the truck, however, there is no information about its loaded state. So the radar can not provide exact in-

formation about the kinetic energy of the vehicle approaching from behind.

5. Impact without pre-braking

Driving courses often tell drivers to keep an eye on the movement of the vehicle behind them in the event of an unexpected breaking event, so they can be prepared for a collision if necessary. In the case of vehicles with automatic transmission, in almost 100% of cases, (and also in the case of manual transmission vehicles), very often the driver depresses the brake pedal while waiting at an obstacle or a lamp. This pre-braked mode strongly influences the course and the effects of the accident. **Figure 6.** shows the impact situation, where the service brakes in the front vehicle
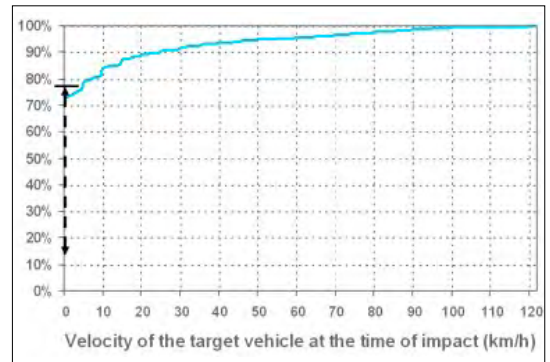
Figure 4. *Statistical data of the frontal vehicle's velocity at the moment of rear impact.* **[5]**
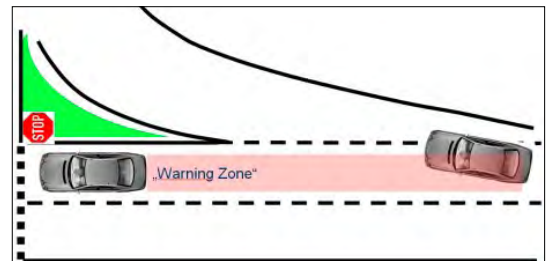
Figure 5. *Over-calibrated radar.* **[5]**
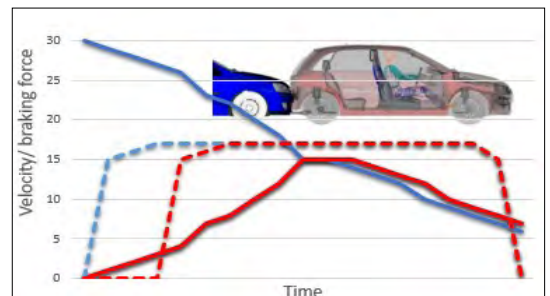
Figure 6. *Collision without pre-braking.*

(coloured red) are not actuated at the moment of impact. The front vehicle at the moment of impact experiences a shock-like, sudden acceleration which results in steep-increased velocity characteristics. The speed of the rear (blue) vehicle sudden reduces to zero, so the deceleration steeply rises and results in a huge impact force on the passengers.

The sudden acceleration of the frontal vehicle can result in whiplash injury in the case of the passengers. If, at the moment of impact, the head is not supported by the head restraint, the head will tilt backwards due to its inertia and, depending on the distance between the head restraints, may suffer even a maximum negative state of so-called hyper-extension. (**Figure 7**)

As **figure 6** also confirms, the participant vehicles decelerate to a common speed point, and then reach zero. This means that passengers in the vehicle in front are burdened with a sudden acceleration at the moment of the collision and then a sudden deceleration from braking due to a defensive or panic reflex. From the state of hyper-extension, the head tilts forward due to the inertia of the head, but depending on the amount of deceleration caused by the sudden stop, even the state of hyperflexion can be reached. This means that the cervical vertebrae and the neck stiffening muscles can suffer from the two anatomical border states in an extremely short time.

6. Reduce whiplash damage with an active headrest

Many recent investigations confirm that the severity of whiplash injury is strongly influenced by the head-headrest distance. According to the proportional nexus, the higher distance results in higher neck and spine injury. **[8–11]**

In accordance with the listed studies in the headrest-supported head case, the severity of the neck injury can be significantly reduced due to the lack of tilting of the head. Based on this, it could be a good solution if the driver adjusts the headrest exactly, as close as possible to his/her head. However, this could cause an uncomfortable driving position and result in further concentration problems. This problem can be reduced by an active headrest. At the moment of rear impact, the headrest moves forward automatically by a spring mechanism and prevents the tilting of the head. (**Figure 8**) With this, the safety and comfort requirements are completed simultaneously.
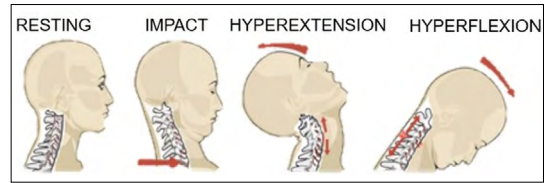
Figure 7. *Movements due to the inertia of the head from the moment of impact.* **[7]**
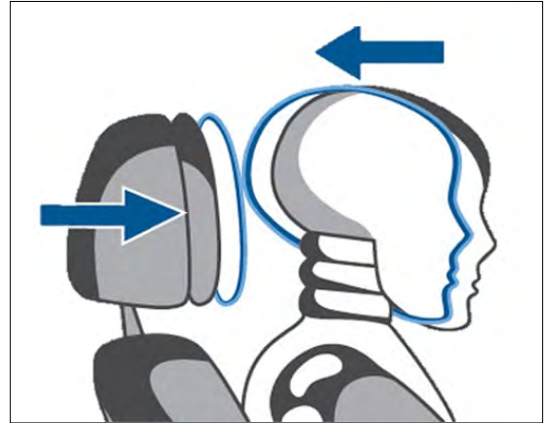
Figure 8. *The function of the active headrest.* **[12]**

7. Impact energy absorption with braking

An object in motion has kinetic energy depending on its mass and speed. In the case of a moving vehicle, the kinetic energy can be converted into thermal energy by braking, so that the speed is reduced to zero. In the event of a collision, this kinetic energy is converted into collision energy. The force generated at the moment of collision works on the displacement projected to deform the crumple zone of the vehicle and is expressed as impact energy. This energy can be absorbed through passive safety elements, thus reducing the amount of impact force on the occupants of the vehicle. During the investigation, we recognized the possibility of applying brake-assistants as an impact energy absorber. It means that we would like to solve passive safety tasks with active safety technologies.

In a panic situation, the drivers actuate the brake pedal fast enough, but not as effectively. This pedal-control crisis is even more complicated if the accident is a rear-end collision, and the passive acceleration is to be be controlled. Furthermore, investigations confirm the fact, the legs of the drivers are displaced from the pedals at the moment of the rear-end impact. (**Figure 9**).

So the driver can not constantly control the braking force to cushion the acceleraion caused by the impact. Furthermore, the lack of a constant brake force could result in a third collision with the previous object. Therefore the in-vehicle applied brake assistant has an important role in terms of active and passive safety also.

7.1. Short review about the brake assistant

The most important parameter for the operation of the brake assist is the operating speed of the brake pedal. The internal structural displacement of the brake assist can be measured with a linear potentiometer. The pedal velocity can be expressed by the time derivation of its displacement. The brake pressure value thus obtained is compared by the electronics of the brake assist with a threshold value currently assigned to the motion parameters of the vehicle (**Figure 10**). The logical operation of the system is accompanied by a self-learning algorithm that determines the deceleration associated with the movement of the brake pedal for each brake application. If the brake assists control electronics detect emergency braking, it immediately activates the brake assist actuator and creates a higher braking force than the current brake pedal depression position. Thus, with the use of the brake assist, deceleration with the same dynamic time as with a strong brake pedal can be achieved, even in the event of an inadequate reaction time or under-braking. With the electrically controlled brake assist the brake effect freely could be modified independently from the driver. Over this control the active brake assist can be utilized in more subsystem operation:

– on an incline, the start can be made free of rolling back,
– suitable for ASR, EDS and ESP control to create pressure when braking,
– allows tracking distance with cruise control or radar sensor control system from the driver implementation of independent deceleration,
– immobilizer in case of theft.

Naturally, these require additional units to supply the system **[13]** We aim to use this braking assistant to overcome this driving behaviour for safety purposes in our development.

7.2. Brake assistant optimization for passive safety

It is very important that in case of a rear accident the vehicle is able to control automatically the brake force during the whole accident event.
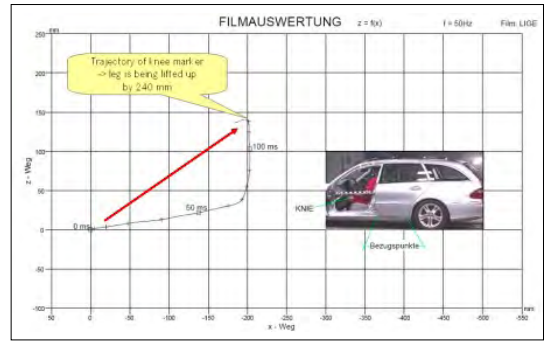
Figure 9. *The displacement of the leg at the moment of rear impact.* **[5]**
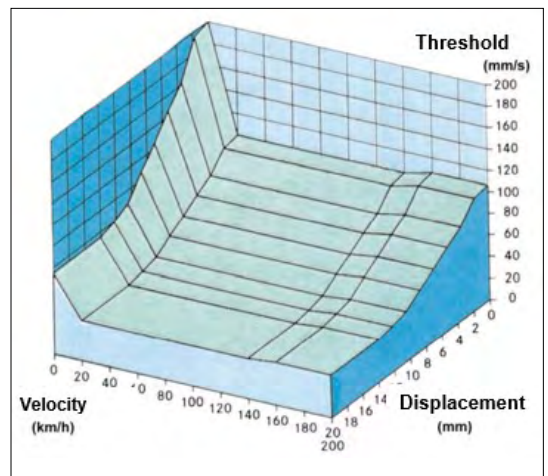
Figure 10. *Operation threshold.* **[13]**
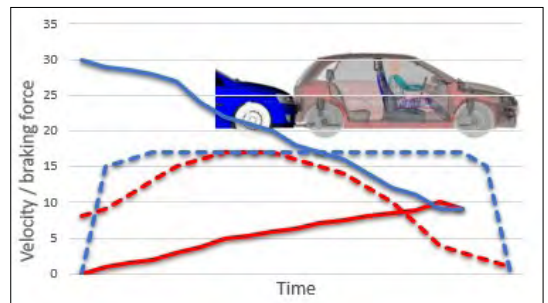
Figure 11. *Moderately pre-braked impact.*

The optimized brake chart for the passive safety is introduced in **Figure 11.** The continuous lines indicate the acceleration and deceleration of the participant vehicle, while the dashed lines present the actuated braking force limit. The colours of the chart lines correspond to the colours of the vehicles shown in the figure.

The basis of the operation is a middle-limited radar, which is mounted behind the rear bumper shell. When the vehicle is stationary at an intersection or a traffic light, the radar examines the danger zone to the rear. When the radar detects an object arriving at high speed from behind, it actuates the safety system and prepares the vehicles for the impact with the help of the control unit. The control unit calculates the necessary pre-braking force for the wheels considering more sensor-supported information. Such data include the presence and distance of an obstacle in front of the vehicle. Since this distance limits the energy absorbed by pre-braked cushioning. In addition, the amount of braking force currently applied by the brake pedal is also important information. The current brake pedal force and the mode of the gearbox are also important information to the proper operation of the safety system. The system could work even more precisely if the rear radar would be able to recognise the size of the arriving vehicle from behind. Since with this information the kinetic energy of the rear vehicle could be calculated before the moment of impact. So from the calculated kinetic energy, the amount of the impact energy can be determined. The brake assistant actuates the proportional braking force with the amount of the kinetic energy according to the control unit calculation. On the wheels, actuated braking force prevents the impact caused by sudden passive acceleration, so the negative, hyper-extension period of the whiplash effect can be reduced. The acceleration of the front vehicle and the deceleration of the rear vehicle can be influenced by the amount of the pre-braking force. So the time of the accident can be expanded, which involves the reduction of the acceleration and deceleration caused by impact force suffered by the passengers. The brake assist must remain operational throughout the impact. The onset of a whiplash injury is positive, so the hyper-extension phase is caused by a sudden stop due to panic braking. In contrast, the safety system based on the brake assist we imagine reduces the increased braking force in the initial phase of the accident, so that the inertia of the head movement can be controlled. The aim is therefore to absorb a significant part of the kinetic energy of the vehicle coming from behind and thus of the impact energy with controlled braking, in addition to the energy absorption caused by the deformation of the creased zones. As shown in **figure 10** at the moment before the collision, the wheels of the vehicle in front are subjected to a moderate

braking force by the brake assistant (dashed red line) This moderate braking force allows the vehicle to roll forward due to the collision, but the extent and acceleration of this forward rolling is limited, while at the same time damping the kinetic energy of the rear vehicle. Compared to a fully blocked pre-brake, this solution also reduces the deceleration of the rear vehicle, thereby reducing the risk of personal injury

7.3. Auxiliary safety devices

In addition on the pre-braking, the pretension of the seat belts could be occurred in response to the signal of the seat occupancy sensor. With this method the body displacement due to inertia could be reduced or prevented. With the possibility of using active headrests, the head can be under-set as early as the moment of impact, thus preventing the head from tilting backwards

7.4. Limitations of a brake assist system optimized for passive safety

Of course, there can be limits to the application of impact energy absorption by braking. Such a barrier may be the detection of an obstacle in front of the vehicle or its proximity. After all, the impact energy absorption is based on the controlled displacement of the vehicle, which requires a displacement phase. The ACC radar already mentioned in the previous chapter provides information on the extent of the available displacement distance. The distance it perceives must be taken into account since a nearby obstacle can partially or even completely sabotage the possibility of displacement, while a distant or unobstructed path allows greater displacement. If an obstacle is detected too close, the solution may be to brake the wheels completely and thus avoid further indirect collisions. Another limitation of the impact energy absorption based on the operation of the brake assist may be the movement of the innocent vehicle. After all, in the case of a small speed deviation, the braking of the vehicle in front to absorb the impact energy can have the exact opposite effect and a collision can occur. In this respect, the application of the safety system described by us is limited primarily to the situation of a collision with a stationary vehicle

8. Conclusions

The focus of our research is on enhancing the collision safety of motor vehicles by applying an active and passive safety system simultaneously. Our study focuses on the absorption of impact

energy from braking by a brake assist. The most common type of crash is that the damage to the whiplash can be traced back to the extraordinary acceleration and abrupt stop caused by the collision. The severity of the injuries can be reduced if the time of the collision can be increased. Based on the vehicle's radar technology, the wheels are braked with a moderate braking force at the moment before the collision. Due to this, the movement of the vehicle in front is allowed, but it is controlled if we want to absorb some of the impact energy with the help of the braking system and prolong the time course of the collision. Nowadays, car manufacturers apply similar solutions to reduce the effect of the rear accident. They use the active brake-based safety system for rear-end collisions, however, they apply the total blocked wheel method at the moment of the accident. Thanks to this, the displacement and the acceleration of the frontal vehicle are almost zero. However owing to the energy conversation law, the impact energy will be handed over to the rear vehicle. This implies more personal and technical injuries at the rear vehicle. According to this scenario, the impact results in serious personal injury and technical damaged by the deceleration force. With belt tensioners and an active head restraint activated at the same time, the extent of injuries can be further reduced.

References

[1] Kőfalvi Gy. Ignácz F.: *Utasmozgás vizsgálata gépjárművek ütközésénél.* Biomechanica Hungarica IV/1. (2011) 19–29.
https://doi.org/10.17489/biohun/2011/1/03

[2] Kőfalvi Gy.: *A gépjárművek aktív és passzív biztonsága.* IbB Hungary.

[3] Tettamanti T., Varga I.: *Az autonóm járművek forgalmi hatásai: a jármű- és forgalomirányítás kihívásai.* A Magyar Tudomány Ünnepe, 2018.
https://doi.org/10.24228/KTSZ.2019.1.4

[4] NHTSA report – *Crashes, by First Harmful Event, Manner of Collision, and Crash Severity.* 2019

[5] Bogenrieder R., Fehring M., Bachmann R.: *Pre-Safe® In Rear-End Collision Situations.* Germany Paper 09-0129

[6] Haight S. H., Haight R.: *Analysis of Event Data Recorder Delta-V Reporting in the IIHS Small Overlap Crash Test, Collision.* The International Compendium for Crash Research, 2013.

[7] Brownlee R.: *Whiplash - Neck Injury.* Welcome Back Clinic - MRI and Pain Management Centre https://www.welcomebackclinic.com/blog/Whiplash---Neck-Injury.htm (2021.11.16.

[8] Ruedemann Jr. A. D.: *Automobile Safety Device-Headrest to Prevent Whiplash Injury*, 1957, JAMA. 164/17. (1957) 1889.
https://doi.org/10.1001/jama.1957.62980170001006

[9] Viano D. C., Gargan M. F.: *Headrest Position during Normal Driving: Implication to Neck Injury Risk in Rear Crashes.* Accident Analysis & Prevention, 28/6. (1996) 665–674

[10] Giorgetta F., Gobbi M., Mastinu G., Ravicino R.: *Developing a 'No-Whiplash' Headrest.* International Journal of Vehicle Systems Modelling and Testing. 4/3.

[11] Diem W.: *Anti-Whiplash Systems.* AutoTechnol, 1. (2001) 44–45.
https://doi.org/10.1007/BF03246590

[12] CBT, What is An Active Headrest & How Does It Work? (2021.11.16)
https://carbiketech.com/active-headrest

[13] Kőfalusi P.: *Fékasszisztenssel rövidebb a fékút – a fejlesztések kezdete.* Autótechnika 2004/10. 24–27.

PARTIAL EXAMINATION OF THE DESIGN OF THE BOMBED OLT BRIDGE IN SÂNCRĂIENI

Zsombor KISFALUDI-BAK,[1,2] F.-Zsongor GOBESZ[3]

[1] Transylvanian Museum-Society, Department of Technical Sciences, Cluj-Napoca, Romania, kisfaludi.zsombor@eme.ro,

[2] Technical University of Cluj-Napoca, Department of Structural Engineering, Cluj-Napoca, Romania, zsombor.kisfaludi@mecon.utcluj.ro

[3] Technical University of Cluj-Napoca, Department of Structural Engineering, Cluj-Napoca, Romania, go@mecon.utcluj.ro

Abstract

Throughout Transylvania, the ruins or remains of many engineering structures and buildings can be observed, and this allows us to draw a lot of interesting conclusions. This research seeks to shed some light on the design process of older bridges in Transylvania through a case study. Hydraulic calculations based on field measurements show the hydraulic requirements used in the original design of the bridge. The obtained data was compared to the current requirements of the Romanian design standards.

Keywords: technical history, bridge design, flood .

1. Introduction

The subject of our topic is the old Olt Bridge in Sancraieni, which was blown up in September 1916 by the retreating Austro-Hungarian army. The original plans of the bridge are not known, but the structure is not unique on the Olt River, similar bridges were built in Sântimbru, Sfântu Gheorghe and in other places. A postcard illustrating the original state of the bridge can be seen in **Figure 1**. Although the superstructure of the bridge (truss, deck and barriers) was completely destroyed, no damage was caused to the two abutments (**Figure 2.**), thus an impromptu pedestrian bridge was made with their help (**Figure 3**).

The only road bridge in the settlement is located 200 meters from the remains of the old bridge on the county road marked 123A. The technical overhaul of the new bridge and the start of repair work are due to begin in the near future, so flood control of the remains of the bombed-out bridge has become increasingly important.

Figure 1. Postcard illustrating the former Olt bridge in Sâncră0ieni, before 1916 **[1]**

Figure 2. Ahe current state of the abutment

Figure 3. *Pedestrian bridge on the original substructure*

2. River section analysis

The subject of this analysis is the cross section of the Olt River in Sancraieni, where the old bridge illustrated in **Figure 1.** was located.

At a distance of 180 meters in front of the cross section of the old bridge is a hydrometric station, the known measurement data of which greatly helped the accuracy our hydrological calculations.

Table 1. *Long-term average flow in the analysed cross section* **[2]**

River	Cadastral number	Average flow
Olt	VIII.1	5,74 m³/s

Table 2. *River parameters in the analysed cross section* **[3]**

Parameter	Value
Length	58 km
Average slope	1.5 %
Sinuosity	1.26
Retention area	902 km²
Average altitude above sea level	644 m

Using the above data, based on the hydrological calculations performed, the resulting maximum flows of the river in its cross-section under the bridge are shown in **Table 3.**

Table 3. *The maximum flows of Olt River in the bridge cross section*

| Qmax	
%	**m³/s**
1	406
5	219

2.1. Current cross section

Following the field measurements, the current cross-section of the riverbed under the position of the former bridge are as shown in **Figure 4.**

2.2. Regenerated, original cross section

A large amount of sediment deposits can be seen in the current cross section of the riverbed, which can be attributed to the constructions in the river channel in front of the old bridge. Based on the geometry of the intact abutments and the level of the riverbed, the cross section presumably taken into account in the design of the bridge is shown in **Figure 5.**

3. Design specifications

Based on Romanian standardization, the flow value used in the design of bridges is selected depending on the priority classification of the structure, according to standard 4068/2 **[4]**. The bridge we examined belongs to priority class 4, according to standard 4273 **[5]**, so the flow value corresponding to the 5 % probability of flood water flow was considered for the calculations.
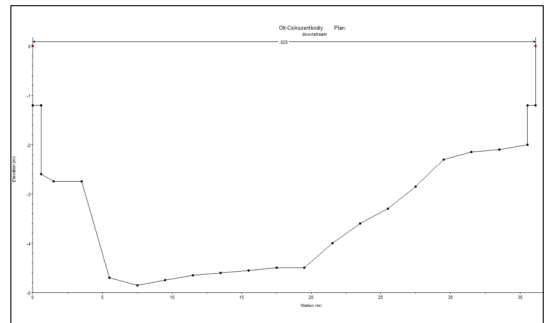
Figure 4. *Current cross section of Olt River at the remains of the old bridge*
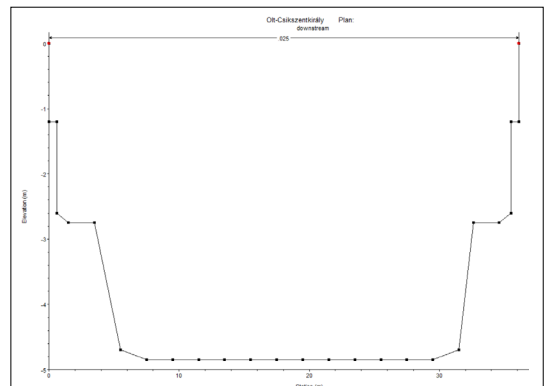
Figure 5. *Assumed original riverbed cross section*

A 2010 government decision stipulates that the target set on the basis of the national strategy for the future is to ensure that the design flow value in rural settlements should be the one corresponding to a 1 % probability of flood water flow [6].

When determining the flow section of the bridges, a certain free height must be taken into account, which, according to the Romanian PD-95 standard, in our case means a height of 1.5 meters [7].

4. Hydraulic calculations

The modelling was carried out using the HEC-Ras software of the US Army Corps Engineers, which uses the Chézy-Manning hydraulic model.

With the help of a first model, we examined whether the bridge, designed more than 100 years earlier, met the pre-2010 Romanian standards, and also whether it meets the current standards..

Based on the results, we can state that the original cross-section meets the requirements of both pre-2010 and post-2010 Romanian design standards. In the case of a maximum flood flow with a probability of 1%, the free height is 2.03 meters (**Figure 6**).

With the help of a second model, the current cross section of the river was investigated for the maximum flood flows mentioned before.

As can be seen from the results shown in **Figure 7,** the current cross-section no longer provides the required free height in the case of a maximum flood flow of 1 % probability.
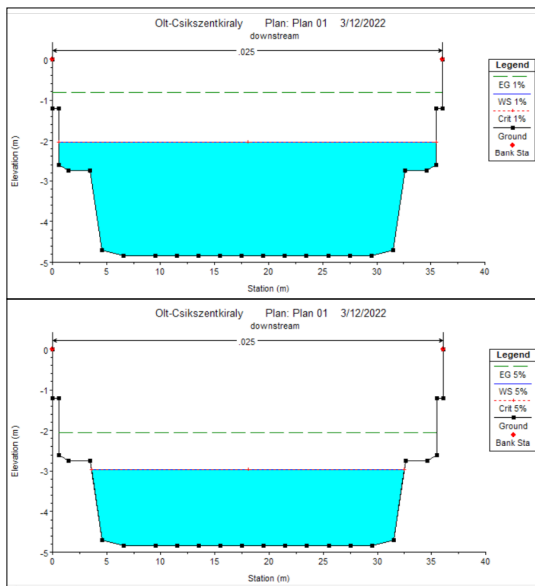
5. Conclusions and further plans

Hydraulic calculations based on the remains of the bombed-out bridge in Sancraieni clearly show that the standards used in the design of the original bridge were stricter, not only by the Romanian regulations valid until 2010, but even by the current standards, thus ensuring the required free height even in case of a 1% probability maximum flood flow, so the newly built pedestrian bridge made on the old abutments meets the requirements of the current Romanian design standards from a hydraulic point of view.

Our second conclusion is that the current riverbed cross-section does not provide the free height required by the standards, and therefore it is necessary to remove the deposited bed sediment shown in **Figure 8.** and to stabilise the riverbed.

Our further plans include the search for and examination of the remains of similar ruined Transylvanian bridges in order to determine the original design requirements.

Acknowledgments

Figure 6. *Assumed original cross section with 1 % and 5% probability maximum flood flows*
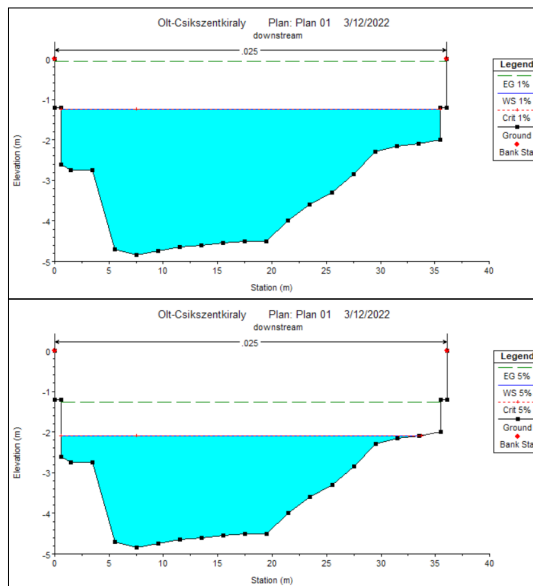
Figure 7. *Current cross-section with 1 % and 5 % probability of maximum flood flows*

Figure 8. *Islands created by riverbed deposits*

References

[1] Private collection of a local resident.

[2] Ministerul Mediului și Dezvoltării Durabile - *Studii pentru cunoașterea resurselor de apă în vederea fundamentării planurilor de amenajare ale bazinelor / spațiilor hidrografice, Bazinul hidrografic Olt.* 2008.

[3] Ministerul Mediului – *Atlasul cadastrului apelor din România, Partea 1 – Date morfo-hidrografice asupra rețelei hidrografice de suprafață.* 1992.

[4] STAS 4068/2-87: *Debite și volume maxime de apă. Probabilități teoretice ale debitelor maxime în condiții normale și speciale de exploatare.*

[5] STAS 4273-83: *Construcții hidrotehnice. Încadrare în clase de importanță.*

[6] HG 846-2010: *Strategia națională de management al riscului la inundații pe termen mediu și lung.*

[7] PD 95-2002: *Normativ privind proiectarea hidraulică a podurilor și podețelor.*

sciendo

EME · MTSZ
MTK

STUDY OF THE EFFECT OF SOIL VOLUMETRIC WEIGHT ON THE ENERGY REQUIREMENT FOR A SPADING MACHINE BY SIMULATION

Judit PÁSZTOR,[1] Ferenc TOLVALY-ROȘCA,[2] Zoltán FORGÓ[3]

[1] Sapientia Hungarian University of Transylvania, Faculty of Technical and Human Sciences, Târgu Mureş, Department of Mechanical Engineering, Romania, pjudit@ms.sapientia.ro

[2] Sapientia Hungarian University of Transylvania, Faculty of Technical and Human Sciences, Târgu Mureş, Department of Mechanical Engineering, Romania, tferi@ms.sapientia.ro

[3] Sapientia Hungarian University of Transylvania, Faculty of Technical and Human Sciences, Târgu Mureş, Department of Mechanical Engineering, Romania, zforgo@ms.sapientia.ro

Abstract

In this paper, we simulate the operation of a spading machine on three soil types; easy to work, medium to work and heavy, using a previously validated SimuLink model of an MSS-1.40M spading machine. We determine the forces during spading. We explore the physical and mechanical properties of the soil that play a role in the spading process. By simulation of the spading process with the MSS-1.40M spading machine, we determine the torque on the drive shaft and the required mechanical work on the three soil types.

Keywords: spading machine, soil volumetric weight, simulation.

1. Introduction

The physical and mechanical properties of the soil influence the energy consumption and the energy required by the tillage machine, at the same time the work of the tillage machine changes depending on the physical and mechanical properties of the tilled soil.

During tillage the soil is rotated, loosened, crushed, mixed, compacted and surface-formed. The tillage work can be classified into basic work and seedbed preparation.

Basic tillage work is a rotation operation, the deepest soil work. This process is most energy intensive.

The basic tillage work in greenhouses is carried out with the spading machine [1], [2]. The spading machine mimics the work of the spade; turns, shreds, loosens and mixes the soil.

The spading machine is an active tillage machine. Its implements are spades, which, in addition to towing, are also driven by the tractor's PTO shaft. Because of this, it has a high specific energy requirement yet less traction requirement. The area performance of PTO-driven tillage machines is not advantageous, but they produce better results in fuel consumption and soil shredding [3].

Determining the energy demand of soil tillage at the frontier of energy and agricultural sciences is always timely [4], [5].

Soil is a complex, open dynamic system that results from the interaction of soil-forming factors and tillage. The soil affects the machines, but the machines also affect the soil [6]. this paper we examine the energy required of spading on different soil types. The energy required for digging is determined by simulation for three soil types.

A simulation is a study in which the process is studied using a computer model. Scientific modelling is playing an increasingly important role in the study of the tillage process and in the scientific approach to the tillage process [7].

2. Work and method

For our study we use a real spading machine model, the MSS-1,40M, and a previously validated SimuLink simulation [8].

We explore the physical, mechanical properties of the soil that play a role in the spading process. Based on the literature [8], we determine their values for soils that are easy to cultivate, moderately cultivable and difficult to cultivate [8].

Following that, we simulate the spading process on the three soil types.

The values of the moments and the required mechanical work during the spading process on the studied soils are determined.

2.1. The MSS-1,40M spading machine model

The assembly model was built using Autodesk Inventor software based on the actual dimensions of the MSS-1.40M spading machine [8].

The simplified assembly model (**Figure 1**) shows the spades, the arms of the spades, the frame of the machine, the parts of the drive shaft, and the two sliders involved in adjusting the working depth.

The trajectory of the tip of the digging edge can be determined by motion simulation (**Figure 2**).

The trajectory provides an opportunity to illustrate the movement of the spade in the soil and to study the work of the spade.

The four stages of the spading work (**Figure 2**) [9]:
– the spade penetrates the soil and cuts the soil chip, A-B;
– the spade separates the soil chip from the soil, B-C;
– the spade raises the soil chip, C-D;
– the spade moves to a new position while the raised soil strikes the cover plate, D-A.

With the trajectory, the forces manifested on the spade can be identified (**Figure 3**) [8]:
– on part A-B, bit force: F_b;
– in section B-C shear force: F_s;
– on section C-D inertia force: F_i.

The following formulas were used to calculate the acting forces [8], [10]:

$$F_b = 2k_1A_1 \, [\sin \beta/2 + \mu \cos \beta/2] + 2\mu k_2 A_2 \; \text{[N]}, \quad (1)$$

$$F_s = s \, l \, \tau = s \, l \, (c + \sigma \tan \varphi) \; \text{[N]}, \quad (2)$$

$$F_i = V \rho \, a_s \; \text{[N]}, \quad (3),$$

where:
- A_1 is the active surface of the spade edges [m²];
- A_2 is the surface of one of the sides of the spade, in contact with the soil [m²];
- β is the lip angle of the spade [°];
- μ is the friction between the soil and the spade;
- φ is the internal friction angle of the soil [°];

k_1, k_2 are the specific resistance to soil deformation [N/m²];
- c is the cohesion of soil [N/m²];
- σ is the surface pressure [N/m²];
- τ shear tension [N/m²];
- s is the spading step [m];
- l is the working length of the spading edge [m];
- V is the volume of the lifted soil chip [m³];
- ρ is the soil volumetric weight [kg/m³];
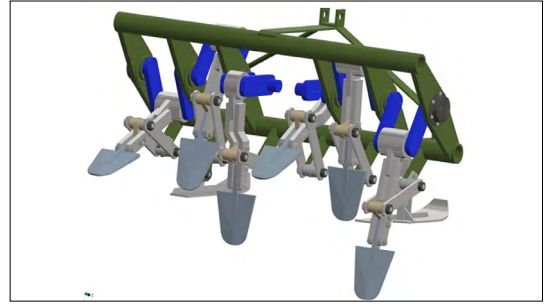- a_s is the displaced soil acceleration [m/s²].

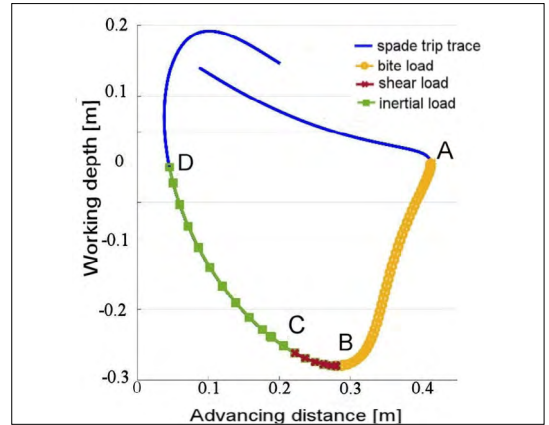**Figure 1.** *MSS-1,40M spading machine assembly model.*

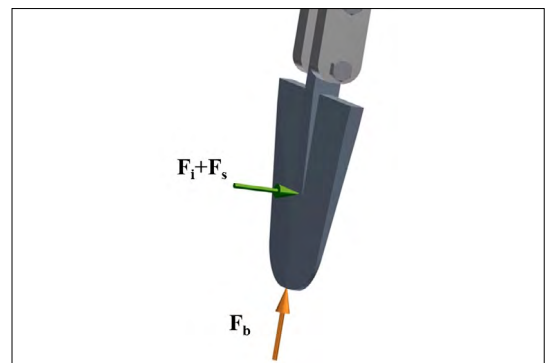**Figure 2.** *The trajectory of the apex of a spade edge.*

Figure 3. *The forces on the spade.*

2.2. Physical and mechanical characteristics influencing spading

The physical and mechanical characteristics of the soil, which play a role in the spading process, can be identified from equations (1÷3):

$$F_b = f(\mu, \phi, k_1(\varphi), k_2(\varphi)) \qquad (4)$$

$$F_s = f(\phi, c, \sigma, \tau), \qquad (5)$$

$$F_i = f(\rho). \qquad (6)$$

The dynamics of spading are affected by:
- μ the coefficient of friction between soil and steel;
- ϕ the internal friction angle of the soil;
- k_1, k_2 the specific resistance to soil deformation;
- c the cohesion;
- σ the surface pressure;
- τ the shear strength;
- ρ the soil volumetric weight.

The physical and mechanical characteristics of the soil depends on the type of soil. The soil types we examined:
- easy to work, sandy loam;
- medium machinable, loam;
- clay loam, that is more difficult to machine.

The values of the physical and mechanical characteristics used in the literature to characterize soil types can be found in **Table 1. [11]**.

Note: The easy-to-use, measurable soil characteristic is ρ, the soil volumetric weight. The soil volumetric weight is the mass of soil in its natural structural state per unit volume. Unit: kg/dm^3, kg/m^3, t/m^3. We accept this as the main feature.

No different data were found in the literature for the value of surface pressure σ for soil types.

Table 1. *Values of soil characteristics used in the simulation*

Soil type	μ	φ [°]	k_1 [N/m^2]	k_2 [N/m^2]	c [N/m^2]	σ [N/m^2]	ρ [kg/m^3]
Sandy loam	0,54	29	$11{,}14 \cdot 10^5$	23943,31	800	20000	1300
Loam	0,61	32	$10{,}96 \cdot 10^5$	24362,71	1000	20000	1500
Clay loam	0,64	38	$10{,}57 \cdot 10^5$	25353,17	1500	20000	1600

2.3. Simulation of the required mechanical work for spading

The required mechanical work for spading was determined using the Simulink simulation. A Matlab ® Simscape ™ model of a spade is shown in **Figure 4. [8]**.

The simulation was performed for the following parameters:
v_m = 0,35 m/s advancing speed;
ω = 17,7 rpm drive shaft spindle speed;
s = 0,124 m spading step;
a = 0,3 m maximum working depth, using soil characteristics corresponding to the three soil types (**Table 1**).

The spading torque requirements for the three soil types were determined. The torque evolution is shown in **Figure 5**.

The spading of loamy clay, the difficult to work soil, has a higher torque requirement.

The simulation was used to determine the values of the mechanical work to be spaded on the six spades during one revolution of the drive shaft. The data are shown in **Table 2.**

The data in the table are shown in **Figure 6.**
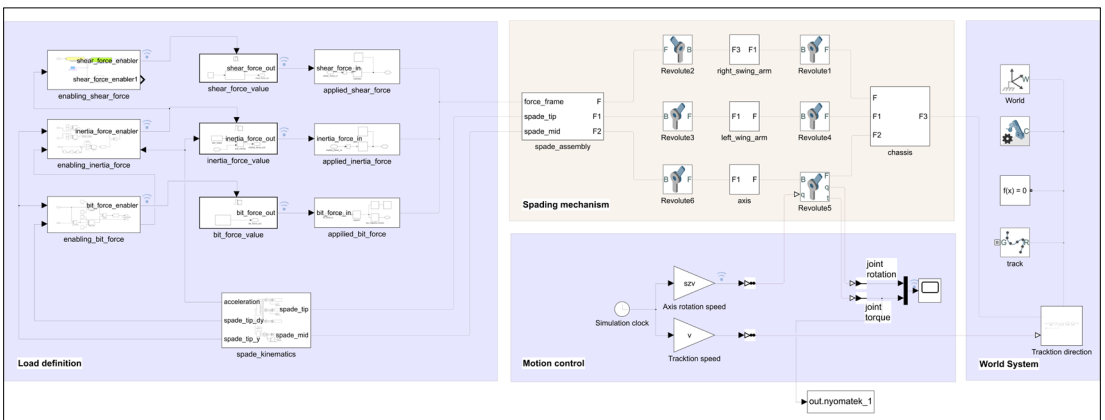
Figure 4. *A Matlab ® Simscape ™ model of a spade.*

The required mechanical work varies during the spading of different soil types (**Figure 6**). The spading of loamy clay soils is more energy intensive.

The correlation coefficient value $R^2 = 0.9833$ in the graph shows a very strong correlation between the soil volumetric weight and the energy requirement for spading.

The equation of the regression line shown in **Figure 6** makes possible to determine the energy requirement for spading with the MSS-1.40M as a function of soil volumetric weight:

$$L = 0{,}12\,\rho - 8{,}92 \quad \text{[J/rev]}. \tag{7}$$

3. Conclusions

The built model describes a working trajectory identical with the others found in the literature, so it can be considered suitable for numerical studies.

The required spading energy, determined using our previous SimuLink model, can be used in the development of cultivation technology and the further calculations of technological cost.

We would also like to apply the presented method to a physical and mechanical soil characteristic that can be determined in the open field. Thus, the energy requirement for the cultivability of a given soil could be estimated on the basis of open field soil characteristic measurements.

References

[1] Giordano D. M., Facchinetti D., Pessina D.: *Te Spading Machine as an Alternative to the Plough for the Primary Tillage.* Journal of Agricultural Engineering, 46/1. (2015) 36–40. doi.org/10.4081/jae.2015.445.

[2] Cardei P., Nuțescu C., Matache M., Cristea O.: *Optimum Working Conditions for Variable Width Ploughs.* INMATEH Agricultural Engineering, 65/3. (2021)248–254. https://inmateh.eu/volumes/volume-65--no-3--2021/article/optimum-working-conditions-for-variable-width-ploughs.

[3] Pezzi F.: *Traditional and New Deep Soil Tillage Techniques in Italy.* American Society of Agricultural and Biological Engineers, 48/1. (2005) 13–17. https://doi.org/10.13031/2013.17935.

[4] Abbaspour-Gilandeh M., Shahgoli G., Abbaspour-Gilandeh Y., Herrera-Miranda M., Hernández-Hernández J., Herrera-Miranda I.: *Measuring and Comparing Forces Acting on Moldboard Plow and Para-Plow with Wing to Replace Moldboard Plow with Para-Plow for Tillage and Modeling It Using Adaptive Neuro-Fuzzy Interface System (ANFIS).* Agriculture, 10/12. (2020) 633. https://doi.org/10.3390/agriculture10120633.

Table 2. *Required mechanical work of spades*

Soil type	ρ (kg/m³)	Required mechanical work (J/rev)
Sandy loam	1300	147.7895
Loam	1500	168.1577
Clay loam	1600	184.6458
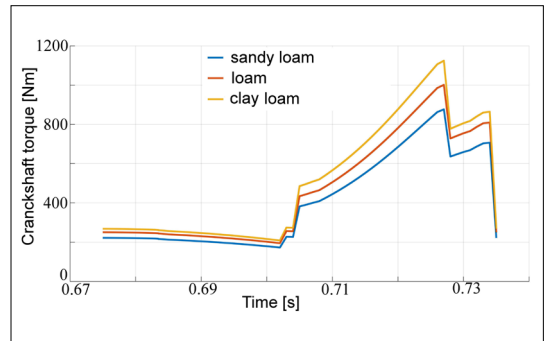
Figure 5. *The torque requirement of a spade during one revolution of the drive shaft.*
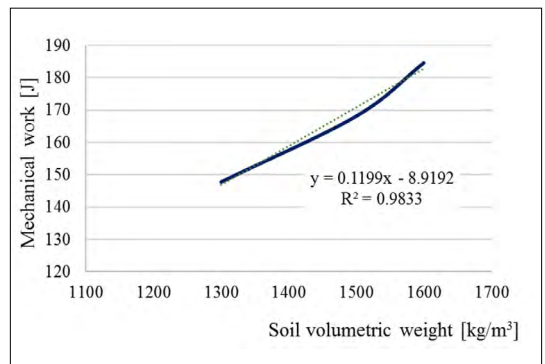
Figure 6. *The relationship between the required mechanical work of spading and the soil volumetric weight.*

[5] Dogra R. Dogra B., Gupta P. K., Sharma B. D., Kumar A.: *Effect of Spade Angle and Spading Frequency of Spading Machine on Specific Soil Resistance and Pulverization.* Agricultural Engineering International: CIGR Journal, 19/1, (2017) 65–73.

[6] Kokieva E. G., Voinash S. A., Sokolova V. A., Gorbachev V. A,; Fedyaev A. A.: T*he Study of Soil Mechanics and Intensification of Agriculture.* IOP Conference Series: Earth and Environmental Science, 548/6. (2020) 1–6. https://doi.org/10.1088/1755-1315/548/6/062036.

[7] Saimbhi V., Wadhwa D., Grewal P.: *Development of a Rotary Tiller Blade Using Three-dimensional Computer Graphics*. Biosystems Engineering, 89/1. (2004) 47–58.
https://doi.org/10.1016/j.biosystemseng.2004.05.011.

[8] Forgó Z., Tolvaly-Roșca F., Pásztor J., Kovari A.: *Energy Consumption Evaluation of Active Tillage Machines Using Dynamic Modelling*. MDPI Applied Sciences, 11/14. 6240. (2021).
https://doi.org/10.3390/app11146240.

[9] Brătucu Gh., Pásztor J., Căpățână I.: *Comparative Researches Regarding the Quality and Efficiency of Germinating Bed Preparing in Greenhouses Through Hoeing and Cutting*. INMATEH - Agricultural Engineering, 31/2. (2010) 63–72.

[10] Máté M.: *Műszaki mechanika – kinematika*, EME Kiadó, Kolozsvár, 2010. 155–163.

[11] Sitkei G.: *Soil Mechanics Problems of Agricultural Machines*. Franklin Book Programs, New York, USA, 1976. 22–62.

REDUCTION OF RETAINED AUSTENITE IN TOOL STEELS

László TÓTH

*Óbuda University, Bánki Donát Faculty of Mechanical and Safety Engineering, Budapest, Hungary,
toth.laszlo@bgk.uni-obuda.hu*

Abstract

Tools are devices for machining materials which must have different properties depending on their intended application. These properties are determined by the chemical composition and microstructure of the tool steel. The desired steel microstructure can be achieved with suitable heat treatment technology. During this heat treatment, the microstructure of the tool steel may develop various lattice structural transformations which in turn can cause internal stresses, cracks and distortions. One possible reason for these undesirable results may be the retained austenite. These effects are most pronounced in tool steels. In this study, the possibilities for reducing the amount of residual austenite during the heat treatment of tool steel is investigated.

Keywords: *tool steel, heat treatment, retained austenite, high tempering temperature, subzero treatments.*

1. Introduction

Tool steels are high alloy steels of controlled chemical composition, the developement of which seeks to yield properties that are suitable for machining and forming various materials [1, 2]. The carbon content of tool steels can vary from 0.1 to 2.0 %. It may contain various alloying elements, Cr, Mo, V, W, Co, Ni, but microalloyed elements such as Nb may be present. Tool steels, according to their aplication, are classified on cold work tool steels, hot work tool steels, plastic mould steels and high speed steels. The materials of these groups must have different properties , eg. cold work tools must have high hardness, high wear resistance, but in some cases they even have to provide good toughness. The hot work tool steels, as they operate above 200°C, must also have good heat resistance, heat abrasion resistance and good tempering resistance. In order to achieve these properties, in addition to using the right alloying components, applying high quality heat treatment technology is important [3, 4, 5].

The tool steel raw material is normally delivered in soft annealed conditions, which means that is in an equilibrium state of structure. During tool manufacturing, thermal and mechanical internal stresses are generated inside the material, which can be reduced with stress relieving technology. It is advisable that this be done before the next heat treatment operation, because the structural transformations also produce stresses and distortions inside the material. These stresses, added to the internal stresses generated in the previous operations, can cause cracks or fractures.

The hardening consists of austenitization and quenching by cooling faster than the critical cooling rate. The austenitization consists of heating with different steps named preheatings to equalise the temperature between the surface and the centre of the part and holding it at austenitization temperature to form homogeneous austenite. The heating rate, the austenitization temperature and the holding time are very important parameters as these together affect the austenite grain size and homogeneity. The austenite grain size is important because it can determine the size of the phases and microstructures that form it, affects the properties of the product. Incorrectly defined parameters contribute to increasing the amount of residual austenite [6, 7, 8].

Another factor that determines the amount of residual austenite is the martensit start (M_s) temperature and the martensite finish (M_f) temperature, which depend on the carbon content and the chemical composition of the steel [9]. As tool steels are generally high carbon, high alloyed steels, their austenitic-martensitic transforma-

tion tempeatures are low, in the case of cold work tool steel, high speed steels, and powder metallurgical tool steels it is generally below 180°C, which means that the complete martensitic transformation is below room temperature, so the presence of residual austenite is unavoidable. The residual austenite is the biggest cause of stresses in the material, as it causes changes in density and volume. During toolmaking, three types of stresses are generated inside the material: stress caused by machining such as turning, milling, grinding or cold working, which can be reduced by stress relieving before hardening; thermal stresses caused by temperature differences depending on the cross section of the piece during heating or cooling, and transformation stresses when the phases and microstructure of the steel is transformed and causes volume changes. After quenching , three phases can be formed, ferrite, martensite and residual austenite, all of different volumes. In order to prevent stresses from causing greater damage, such as cracking or breaking, the tool must be tempered as soon as possible after hardening **[10, 11]**.

During tempering, the martensite decomposes, but some of the retained austenite is converted to martensite while the hardness of the steel decreases as a function of the tempering temperature. In the case of steels contaning carbide-forming alloys, the second tempering can be carried out at high temperatures, which can result in carbide precipitation leading to secondary hardening, setting the final hardness. In this case, the martenite is spheroidized and the retained austenite is converted to martensite. The precipitate, secondary carbides make the microstructure more homogeneous and result a toughness material. By using a third tempering, the amount of residual austenite can be further reduced. However , the cryogenic treatment is the most effective method for minimizing the residual austenite content. During cryogenic treatment, the cooling of the tool does not stop at room temperature, it continues at sub zero temperatures using liquid nitrogen **[12, 13, 14]**.

There are several ways to do this. One is when the quenched tool is taken out of the furnace and placed into a refrigerator chamber when the liquid nitrogen is pulverized, thus cooling the air space to minus 80°C. Another method is the "cool plus" technique, where the ware cooling continues in the hardening furnace by injecting pulverized liquid nitrogen into the furnace chamber, thus cooling to minus 150°C. The third method is

when the cryogenic treatment is performed by placing the cooled ware in the liquid nitrogen at minus 196°C. Cryogenic treatment increases the precipitation of secondary carbides, thus improving the toughness of the workpiece as a dispersed, homogeneous distribution, and of course completes the austenite-martensite transformation, thus ensuring the dimensional stability of the product.

In this study tests were perfomed on Uddeholm Sverker 21 high carbon and chromium cold forming tool steels. The specimens to be examined were subjected to three types of heat treatment, after each heat treatment operation, hardness tests were performed, and the different microstructures were examined using an optical microscope.

2. Materials and experimental methods

Uddeholm Sverker 21 is a ledeburitic cold working tool steel with a high carbon content, and alloyed with Cr, Mo, and V carbide-forming elements. Uddeholm Sverker 21 is a tool steel with excellent abrasion resistance, compressive strength, good through-hardening properties, high stability in hardening and good resistance to tempering-back. Highly nitriding and nitrocarburizing. This material application is for bending, deep-drawing, punching, cutting, but can be used as raw material for different knives. The hardness after hardening can reach 64 HRC. In practice after tempering the ususal hardness for use is 54-60 HRC.

The exact chemical composition of the specimen was analyzed with a Hitachi PMI spectrometer (**Figure 1**).

Figure 1. *HITACHI PMI spectrometer*

The chemical composition of the tested Uddeholm Sverker 21 steel specimen is shown in **Table 1**.

The raw material of the specimen was in a soft annealed condition with an average value of 212 HB. The hardness testing machine HPO 250 is shown in **Figure 2**.

The heat treatments were performed in an IU72/1F 2RV 10bar CP type Schmetz vacuum furnace (**Figure 3**), and the tempering treatment in a Muhel type furnace under protective nitrogen gas (**Figure 4**).

After hardening and tempering, the hardness was measured by the Rockwell C method on an ERNST AT 130D hardness tester (**Figure 5**).

The microscopic examinations of the prepared specimens were performed using an Olympus DCX1000 optical microscope (**Figure 6**).

Table 1. *Chemical composition of the investigated steel grades*

	C	Si	Mn	Cr	Mo	V
Sverker 21	1.56	0.33	0.39	11.28	0.78	0.76

Figure 4*. Muhel tempering furnace*

Figure 2. *HPO 250 hardness testing machine.*

Figure 5. *Rockwell C hardness tester machine.*

Figure 3. *Schmetz vacuum furnace.*

Figure 6. *Olympus DCX 1000 optical microscope*

Three types of heat treatment technologies were applied to the specimens. The hardening was performed in the Schmetz type vacuum furnace and the tempering in the Muhel type nitrogen gas protected furnace. In the first case, low temperature (1200 °C) austenitizing and low temperature (190 °C) tempering, in the second case, high temperature (1075 °C) austenitizing and three times high temperature tempering (525, 535, 515 °C) (**Figure 7**), while in the third case, after high temperature austenitizing cryogenic treatment quenching with liquid nitrogen (in minus 150° C) (**Figure 8**) was used, and which was perfomed three times at high temperature (525,535,515 °C) (**Table 2**).

Heat treatment diagram of the sample tempered at three times higher temperature is shown in **Figure 7**.

Figure 7. *Heat treatment diagram of specimen nr.2.*
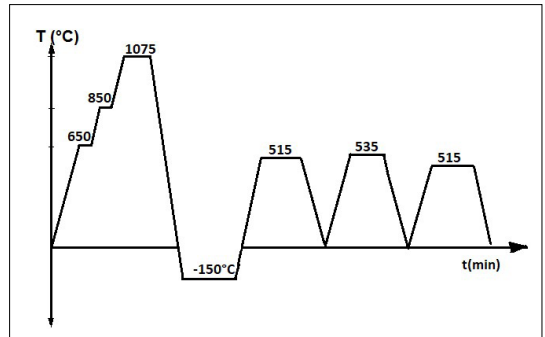
Figure 8. *Heat treatment diagram of specimen nr.3.*

Table 2. *Heat treatment parameters*

Speci-men nr.	Austenitizing (°C/min)	Cryogenic treatments (°C/min)	Tempering (°C/min)
1	650/15 850/15 1020/20	-	190/120
2	650/15 850/15 1075/20	-	525/120 535/120 515/120
3	650/15 850/15 1075/20	– 150/50	525/120 535/120 515/120

3. Results of experimental measurements

Between and after the heat treatment operations, a hardness measurement was performed. The measured hardness values are shown in **Table 3**.

Based on the results of the hardness tests, it can be concluded that the hardness values of specimens 2 and 3 are lower than those of the specimen 1 performed at a low hardening temperature. This is due to the fact that after high temperature hardening some of the primary chromium, molybdenum, vanadium carbides and their complex carbides are dissolved on the matrix and are more residual austenite quantities.

The microstructures of the specimens prepared by grinding, polishing, and etching using 2% Nital solution are shown in **Figures 9.a–c**. It can be seen from **Figure 9.a**, that the amount of primary carbides in the microstructure of low temperature tempered tool steel is quite high, reach-
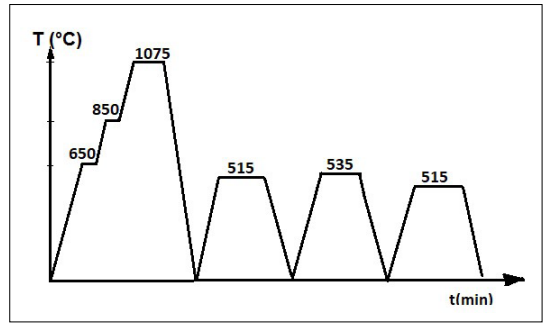
Table 3. *Hardness values after heat treatments*

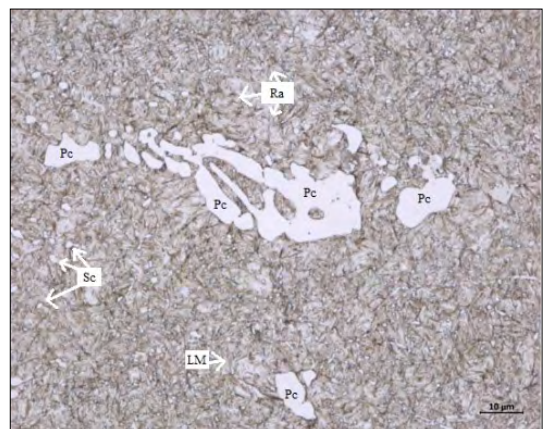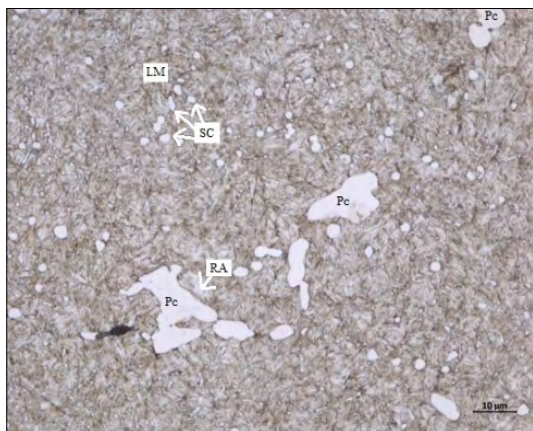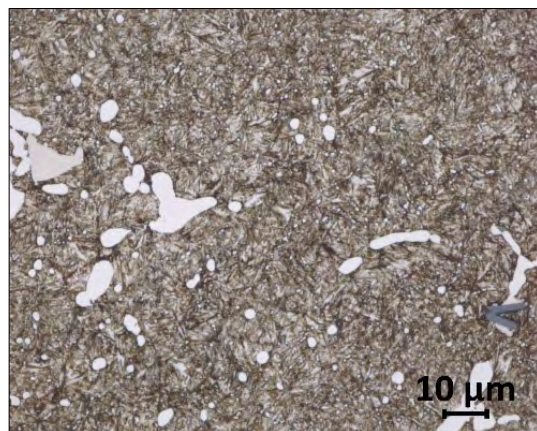| Specimen nr.	Soft annealed (HB)	After hardening (HRC)	After tempering (HRC)
1	212	62	60
2	212	61	60
3	212	61	60

Figure 9.a. *Microstructures of specimen nr. 1.*

Figure 9.b. *Microstructures of specimen nr. 2.*

Figure 9.c. *Microstructures of specimen nr. 3.*

ing 60μm, and the amount of residual austenite reaches 8-10%. The microstructure of specimen nr. 2, which was austenitized at high temperture and tempered three times at high temperatures, shows that a part of the retained austenite was transformed in tempered martensite , and the amount and size of primary carbides were reduced by more than 50%, and at high temperatures precipitated secondary carbides are visible. The **Figure 9.c.** shows at a 1000x magnification a microstructures of specimen nr.3, cooled to minus 150°C and tempered three times at high temperatures . It can be seen that the amount of residual austenite has been reduced to a minimum af about 1 % by cryogenic treatment and the microstructure is characterized by fine, dispersed secondary carbides.

4. Conclusions

Uddeholm Sverker 21 grade is a ledeburitic cold working tool steel with a very good abrasive wear resistance, with good through-hardening properties, good toughness and dimensional stability after heat treatments. After low temperature hardening and one time tempering, a good hardness value was obtained, but the microstructure showed inhomogenity, in the presence of large primary carbides, and caracterised by residual austenite and martensitic structure. Specimen nr. 2 which was austenitized at high temperature and tempered three times at high temperatures, showed a homogeneous, uniform smaller carbide distribution in the microstructures. The amount of residual austenite was reduced to about 4%. Sample nr. 3 was cryogenic treated, resulting in a more dispersed, finer secondary carbide distri-

bution on the microstructures, and the residual austenite was almost undetectabled. Using cryogenic treatment the best toughness properties and the longest service tool life of the product can be achieved.

References

[1] Swamini A. Chopra, V.G. Sargade: *Metallurgy behind the Cryogenic Treatment of Cutting Tools: An Overview*. 4th International Conference on Materials Processing and Characterization. Materials Today: Proceedings, 2/4–5. (2015) 1814–1824.
https://doi.org/10.1016/j.matpr.2015.07.119

[2] Daniel Tobola, Witold Brostow, Kazimierz Czechowsky, Piotr Rusek: *Improvement of Wear Resistance of Some Cold Working Tool Steels*. Wear, 382–383 (2017) 29–39.
https://doi.org/10.1016/j.wear.2017.03.023

[3] A. Oppenkowski, S. Weber, W. Theisen: *Evaluation of Factors Influencing Deep Cryogenic Treatment That Affect the Properties of Tool Steels.* Journal of Materials Processing Technology, 210/14. (2010) 1949–1955.
https://doi.org/10.1016/j.jmatprotec.2010.07.007

[4] Tóth L., Fábián E. R., Huszák Cs.: *Heat Treatment Effects on Properties of K110 Böhler Steel*. Abstracts Book of 10th International Engineering Symposium at Bánki, (2018) 85.

[5] Martin Kurik, Jakub Lacza, Tomas Vlach, Jana Sobotova: *Study of the Properties and Structure of Selected Tool Steels for Cold Work Depending ont he Parameters of Heat Treatment*. Materials and Technology, 51/4. (2017) 585–589.
https://doi.org/10.17222/mit.2016.120

[6] Yaowen Xu, Fei Chen, Zhen Li, Gengwei Yang, Siquian Bao, Gang Zhao, Ximping Mao, Jun Shi.: *Kinetics of Carbon Partitioning of Q&P Steel: Considering the Morphology of Retained Austenite.* MDPI, Metals, 12/2. (2022) 344.
https://doi.org/10.3390/met12020344

[7] Muneo Yaso, Shuhei Hayashy, Shigekazu Morito, Takuya Ohba.: *Characteristics of Retained Austenite in Quenched High C-High Cr Alloy Steels.* Materials Transactions, 50/2. (2009) 275–279.
https://doi.org/10.2320/matertrans.MRA2008161

[8] M. Perez, C. Rodriguez, F.J. Belzunce.: *The Use of Cryogenic Thermal Treatments to Increase the Fracture Toughness of a Hot Work Tool Steel Used to Make Forging Dies.* Procedia Materials Science, 3. (2014) 604–609.
https://doi.org/10.1016/j.mspro.2014.06.100

[9] Gavriljuk V. G, Theisen W., Sirosh V.V.: *Low-temperature Martensitic Transformation in Tool Steels in Relation to Their Deep Cryogenic Treatment.* Acta Materiala, 61/5. (2013) 1705–1715.
https://doi.org/10.1016/j.actamat.2012.11.045

[10] Das D., Dutta A.K., Toppo V., Ray K.K.: *Effect of Deep Cryogenic Treatment on the Carbide Precision and Tribological Behaviour of D2 Steel, Materials Manufacturing* Processes, 22/4. (2007), 474–480.
https://doi.org/10.1080/10426910701235934

[11] Molinari A., Pellizzari M., Gialanella S., Straffelini G., Stiasny K. H.: *Effect of Deep Cryogenic Treatment on the Mechanical Properties of Tool Steels.* Journal of Materials Processing Technology, 118/1–3. (2001) 350–355.
https://doi.org/10.1016/s0924-0136(01)00973-6

[12] Das D, Sarkar R., Dutta A.K., Ray K.K.: *Influence of Sub-zero Treatments on Fracture Toughness of AISI D2 Steel.* Materials Science and Engineering: A, 528/2. (2010). 589–603.
https://doi.org/10.1016/j.msea.2010.09.057

[13] Patricia Jovicevic-Klug, Matic Jovicevic-Klug, Tina Sever, Darja Feizpour, Bojan Podgornic: *Impact of Steel Type, Composition and Heat Treatment Parameters on Effectiveness of Deep Cryogenic Treatment.* Journal of Materials Research and Technology, 14/5. (2021) 1007–1020.
https://doi.org/10.1016/j.jmrt.2021.07.022

[14] D. Senthilkumar: *Effect of Deep Cryogenic Treatment on Residual Stress and Mechanical Behaviour of Induction Hardened En 8 Steel.* Advances in Materials and Processing Technologies, 2/4. (2016) 427–436.
https://doi.org/10.1080/2374068X.2016.1244326

CHROMATIC DISCRIMINATION TOWARDS THE CONFUSION POINTS

Ágnes URBIN,[1] Balázs Vince NAGY[2]

[1] *Budapest University of Technology and Economics, Faculty of Mechanical Engineering, Department of Mechatronics, Optics and Mechanical Engineering Informatics, Budapest, Hungary, urbin@mogi.bme.hu*

[2] *Budapest University of Technology and Economics, Faculty of Mechanical Engineering, Department of Mechatronics, Optics and Mechanical Engineering Informatics, Budapest, Hungary, nagyb@mogi.bme.hu*

Abstract

In this paper chromatic discrimination thresholds of normal colour-observers are analysed. Measurements were obtained with the Cambridge Colour Test, in different reference points. The results show differences in terms of the reference chromaticities. Reference points within the gamut of a CRT display were found where thresholds of normal colour observers measured towards the confusion points exceeded the normative upper threshold limit of normal colour observers. The discrimination thresholds estimated towards the confusion lines based on Trivector measurements exceeded the thresholds estimated by the Ellipse tests. Our results indicate that in case of determination of discrimination ellipses, measurements towards the confusion points are recommended.

Keywords: *chromatic discrimination, confusion point, just noticeable difference, Cambridge Colour Test.*

1. Introduction

A fundamental topic of colour vision assessment is the analysis of chromatic discrimination, which can indicate inherited defects in colour vision, such as anomalous trichromacy [1], early stage of diseases, such as diabetes [2], harmful environmental effects [3, 4] or changes in terms of age [5].

Nevertheless, measurement and analysis of chromatic discrimination are important steps on the scientific road towards the colour differences and the uniform colour spaces, and their verification [6–8].

The measurement method and the experimental design naturally needs to be in accordance with the objective of the actual research. Therefore, during the decades of the history of colour science several methods has been developed and applied for various clinical and investigational aims [9, 10].

One of the most striking beauties of research into colour vision is, ironically, its difficulty; specifically, that colours do not exist without the observer. The human visual system is an elemental part of a system of measurement aiming to study

colour perception and cognition, hence minimizing human error is a great challenge in all measurement methods.

For that reason, although in the literature there are studies about definition and comparison of large colour differences [11, 12], the unit of chromatic discrimination measurements is most usually the just noticeable difference (JND), hence the smallest colour difference which the observer still can perceive.

Several JND measurement methods can be found in literature. In the case of colour matching, the task is most usually to create a colour stimulus as the additive mixture of predefined primary colours matching a target colour, both displayed in separate fields of an aperture. In this case the main parameters are the reference colour stimulus and the primary colours of the mixing light. For colour matching examination a practical example is the anomaloscope, but even MacAdam used this method in his experiment which provides a fundamental database of chromatic discrimination ellipses (known as MacAdam ellipses), which are still widely used as reference in colorimetry [13].

Another prevalent method is colour ranking, where the task is to rank the coloured samples based on one or more colorimetric parameters (most often the chromaticity). In this case the perceptible difference between the successive samples is the main parameter, which can be defined as brightness, saturation, chromaticity, or any combination of these. For this test method two prevalent examples are the FM100HUE and the D15 tests but colour ranking tests are recommended as standard for the validation of normal colour vision of sensory assessors as well [14].

In clinical practice pseudo-isochromatic tests are often used. The main concept in these tests is the design of the test figures, built of randomly sized and positioned dots. Within the figure, the dots can be grouped as target and background, based on their chromaticity, while the lightness of the dots is randomised. The task is to read the target, which is possible only if the perceptible difference between the target and the background chromaticity exceeds the JND of the observer. The most prevalent pseudo-isochromatic test is the Ishihara test [15]. which is designed especially for the detection of two kinds of anomalous trichromacy: deuteranomaly and protanomaly. The main concept of the method is that the chromaticities of the backgrounds and the targets of the test images lie along the Protan or the Deutan confusion lines, therefore anomalous trichromat observers cannot, or hardly can, discriminate them.

Another pseudo-isochromatic test, prevalent in colour vision research is the Cambridge Colour Test (CCT). The advantage of CCT compared to the Ishihara test is that CCT is a computer-based test, so that experimental design can be created beyond the assessment of anomalous trichromacy [16, 17]. The task is to read a Landolt C character from the test figures (see **Figure 1**) and to give its orientation using a remote control. The main parameters of the test are the chromaticities of the background (reference chromaticity) and the Landolt C figure, as well as the range of luminance noise appearing in the figures.

The test is adaptive, the colour difference between the reference chromaticity (unchanged during the test) and the chromaticity of the Landolt C character is continuously increased or decreased based on the subject's responses. This adaptability, as well as the use of a calibrated CRT monitor and the ViSaGe MkII colour stimulus generator, make it possible not only to examine subjects with defective colour vision, but also to
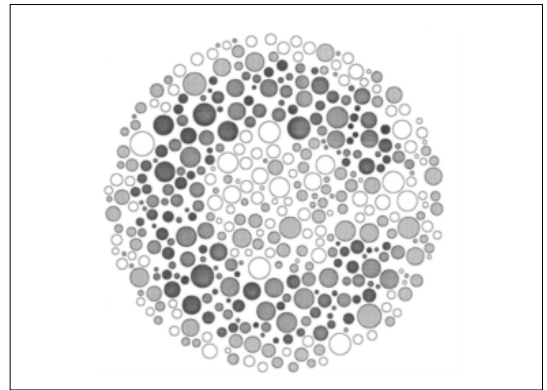
Figure 1. *The structure of a test figure of the Cambridge Colour Test. Darker dots indicate the pattern to be detected, lighter dots indicate the background. In reality, these two areas of the pseudo-isochromatic figure differ in chromaticity instead of lightness* [18].

detect differences in the colour vision of normal colour observers.

The native colour system of the test is the CIE 1976 UCS colour chart, so it gives the chromaticity coordinates as (u';v') coordinates and the thresholds resulting from the measurement as $\Delta E_{u'v'}$ colour differences.

The two test modules of CCT are the Ellipse Test and the Trivector Test. In the case of the Ellipse test, the thresholds are determined in the measurement directions taken in equidistant directions from the reference point, and then, knowing the threshold values and the reference point, the program fits an ellipse using the least squares method to estimate the area within which the observer cannot perceive difference.

The Trivector test gives thresholds from the reference points towards the three confusion directions. Confusion directions are directions from any chromaticity point to one of the three confusion points on the CIE 1931 or 1976 UCS colour diagram. **Figure 2.** shows the confusion directions to the Protan (0.6579; 0.5013), Deutan (1.2174; 0.7826), and Tritan (0.2573; 0.0000) confusion points in the CIE 1976 UCS colour chart.

According to the official guidelines of the CCT [17] in the Trivector test we can talk about defective colour vision for a threshold value exceeding $100 \cdot 10^{-4}$. $\Delta E_{u'v'}$ in the Protan and Deutan confusion directions, and $150 \cdot 10^{-4}$. $\Delta E_{u'v'}$ in the Tritan confusion direction. When evaluating the Ellipse test, colour vision is typically considered normal for an axis ratio below 2.0. The limit values of the normative lower and upper Trivector test results
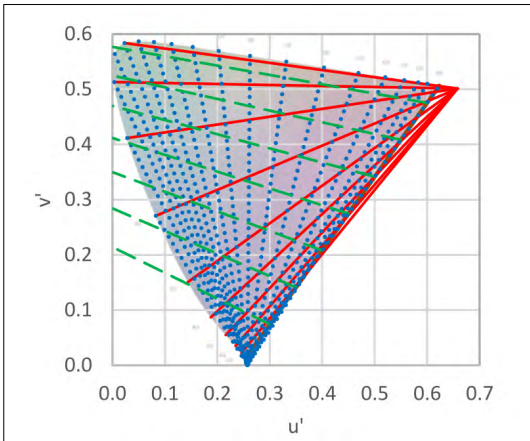
Figure 2. *Protan (solid red lines), Deutan (dashed green lines), and Tritan (dotted blue lines) confusion directions, plotted in the CIE 1976 UCS colour chart.*

determined in the literature [19] in the case of normal colour observers measured at the reference point (0.197; 0.469) are the following:

Protan: $25.2 \cdot 10^{-4}$; $69.3 \cdot 10^{-4}$;
Deutan: $24.7 \cdot 10^{-4}$; $82.4 \cdot 10^{-4}$;
Tritan: $37.3 \cdot 10^{-4}$; $113.4 \cdot 10^{-4}$.

The normative values for the Ellipse test in the following 3 reference points are known for normal colour observers. Field 1: (0.197; 0.469), Field 2: (0.193; 0.509), and Field 3: (0.204; 0.416). Normative values are given as the length of the major axis and the ratio of major to minor axes:

Field 1: $127.7 \cdot 10^{-4} \pm 35.8 \cdot 10^{-4}$; 1.6 ± 0.3;
Field 2: $142.1 \cdot 10^{-4} \pm 38.7 \cdot 10^{-4}$; 1.6 ± 0.4;
Field 3: $174.9 \cdot 10^{-4} \pm 47.7 \cdot 10^{-4}$; 2.2 ± 0.5.

While the purpose of CCT measurements in the literature is typically to compare different groups at the reference points given in the CCT manual [5, 20, 21], little data can be found on the threshold values at reference points that are very different from neutral grey. A study published by the authors of this paper [22] based on a series of Trivector tests performed in a reference point grid covering the entire gamut of a CRT monitor, shows that as the reference points are shifted from the neutral point in a confusion direction, the threshold measured from the shifted reference point in the above confusion direction increases greatly, and this increase can be estimated by a mathematical model.

The aim of our research presented in this paper is to investigate whether the increase in threshold measured towards the confusion directions can also be detected in the case of ellipse tests.

2. Methods

The measurements were performed binocularly by university students with normal colour vision in a darkened room where only the monitor displaying the test was visible. In the test figures, a luminance density of 5 ± 3 cd/m^2 ensured that only a chromatic difference could be detected, and no decisions were made based on luminance difference.

The experimental design is in line with previous research [22]: the neutral point was defined as (0.2024; 0.4689), the reference points were shifted from this point along 8 equally distributed directions.

In the experimental design the following definitions were used: the reference direction is the direction of reference points from the neutral point to the reference point (denoted by: δ); the measurement direction is the direction in which the colour of the Landolt C character changes with respect to the reference point; and ϑ indicates the direction of the major axis of the ellipses. The directions are in each case relative to the u' abscissa.

The reference directions are denoted in the form *(k)* where $k = \delta/(\pi/4)$. The reference points are denoted along the reference directions as a function of reference distances. The reference distance increases along the arrows in the lower right corner of **Figure 3** so that the neutral point is set to 0 along each reference direction. Its unit is $\Delta E_{u'v'} = 0.027$. **Figure 3** denotes the reference points -5, (3) and 3, (3) along the reference direction (3).
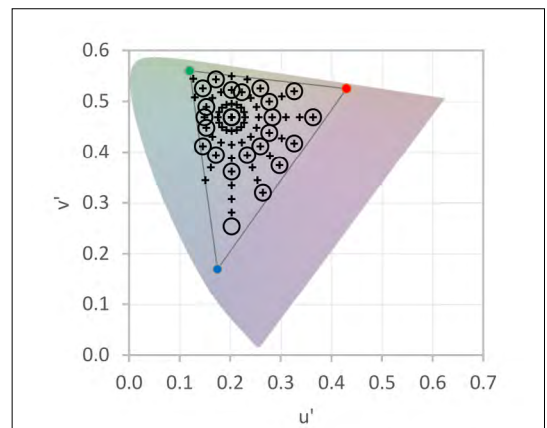
Figure 3. *Reference directions and reference points for the Trivector tests (+) and the Ellipse tests (o) in the CIE 1976 UCS colour chart.*

While the previous Trivector tests were performed in equal steps at a total of 66 reference points, the Ellipse tests were performed at a total of 23 points. Ellipse reference points were also distributed along the gamut of the display. The reference points of both experiments are shown in **Figure 3.**
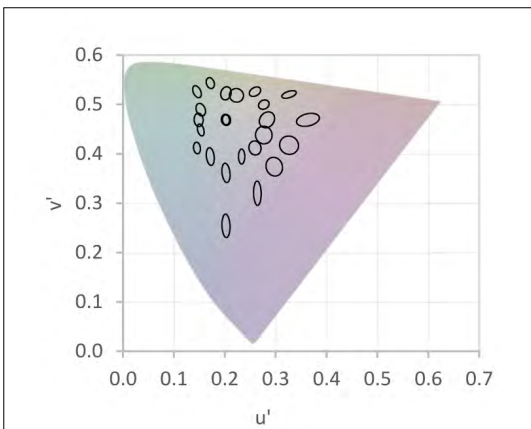
3. Results and evaluation

Ellipse tests were performed with 8 measurement directions. Although the CCT gives the parameters of an ellipse fitted to the measured thresholds as a result of each measurement, ellipses fitted to the mean values of the thresholds measured per reference point were examined by the method of least squares during the evaluation. The resulting colour discrimination ellipses are shown in **Figure 4.** The ellipses are shown at 3× magnification.

A detailed evaluation of Trivector tests can be found in the authors' previous publication **[22]**. The result used in the present research is the estimation of the threshold values (Δ) measured towards the confusion directions with quadratic polynomials as a function of the reference direction and the reference distance based on (1), (2) and **Table 1.** where x is the reference distance.

$$\Delta_{P,D,T} = c_2 \cdot x^2 + c_0 \qquad (1)$$

$$c_2(\delta) = \sqrt{\frac{a^2 \cdot b^2}{a^2 \cdot \sin^2(\delta - \vartheta) + b^2 \cdot \cos^2(\delta - \vartheta)}} \qquad (2)$$

Table 1. *Parameters of equations (1) and (2).***[22]**

	Protan	Deutan	Tritan
a	2.3810	2.1872	4.6203
b	0.5549	0.7265	0.5507
ϑ	171.84°	170.62°	95.57°
c_0	31.4695	31.0190	50.2427

In the confusion directions, the threshold values estimated from equations (1) and (2) and **Table 1** determined from the Trivector measurements, and the corresponding radii of the ellipses obtained as a result of the Ellipse test measurements are shown in **Figures 5** and **6.** In the figures, the hatched dots indicate the Trivector and the filled dots indicate the Ellipse results for the Protan (•) Deutan (♦) and Tritan (▲) confusion directions, respectively. On all three graphs, the abscissa is the reference distance, and the ordinate is the chromatic discrimination threshold.
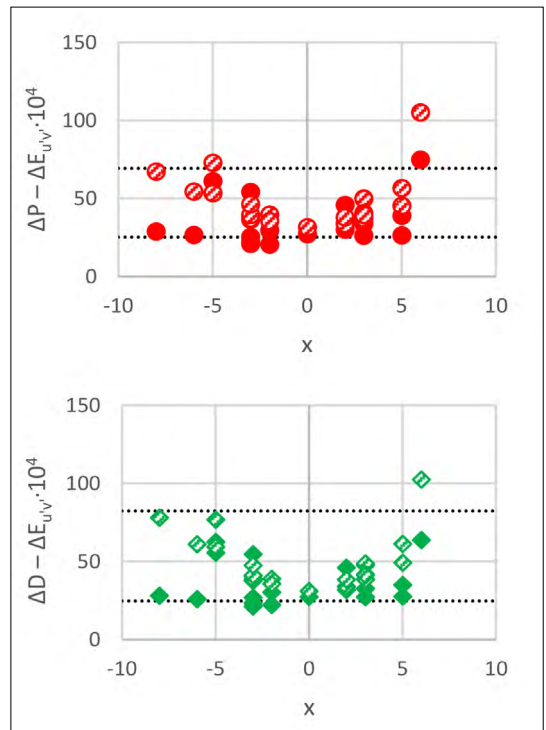
Figure 5. *Estimated chromatic discrimination thresholds (ΔP and ΔD) along the Protan (top) and Deutan (bottom) confusion directions based on the results of the Trivector (hatched) and Ellipse (filled) tests as a function of the reference distance. The dashed lines indicate the expected range of thresholds published in the literature.*

Figure 4. *Chromatic discrimination ellipses in the CIE 1976 UCS colour chart. The ellipses are shown at 3x magnification.*

The direction of the major axes shows a strong, linear correlation with the reference direction (Spearman correlation coefficient: 0.82; p = 1.73E-06, see **Figure 7**), so the colour discrimination ability typically deteriorated along the reference colours of the measurements.
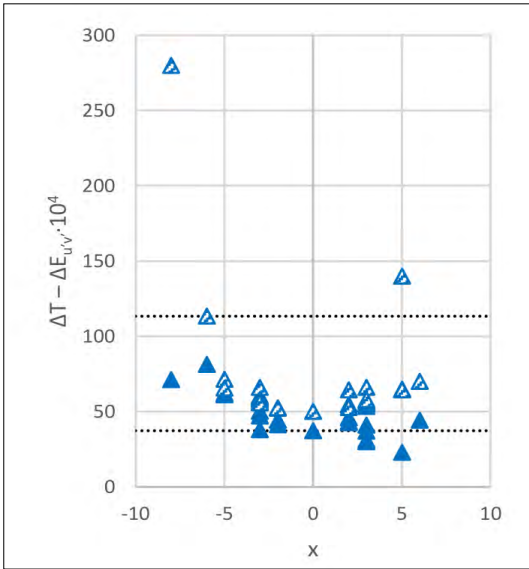
Figure 6. *Estimated chromatic discrimination thresholds (ΔT) along the Tritan confusion directions based on the results of the Trivector (hatched) and Ellipse (filled) tests as a function of the reference distance. The dashed lines indicate the expected range of thresholds published in the literature.*
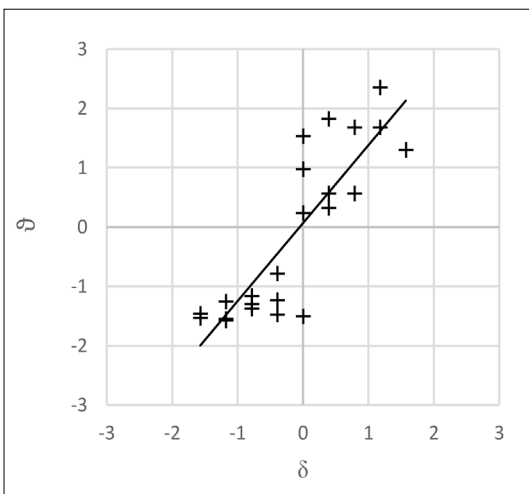
Figure 7. *Direction of the major axis of the ellipses (ϑ) as a function of the reference directions (δ).*

4. Summary, conclusion

Figures 5 and **6** illustrate that the thresholds measured in the Protan and Deutan confusion directions are similar and show a different distribution from the Tritan values for both metrics. For all three confusion directions, threshold values are seen that exceed the upper limit of the chromatic discrimination thresholds of normal colour observers.

Figure 7 and the associated correlation test show that the direction of elongation of the ellipses is strongly influenced by the direction in which the reference point is offset from the neutral colour point in the 1976 UCS diagram. However, the ellipses themselves (see **Figure 4**) show that the ellipses extended toward the Protan and Tritan confusion points, whereas no such direction was observed in the direction of the De-utan confusion point. This may be due to the fact that the gamut of the monitor includes a significantly narrower displayable colour range from the neutral point to the Deutan confusion direction, so we were able to display fewer reference points in the Deutan direction. To investigate this effect, further measurements are required with a display with a wider gamut.

Based on the graphs in **Figures 5** and **6,** the Trivector estimates exceed the threshold values calculated from the Ellipse measurements at the same reference point in almost all cases, so there were colours outside the estimated chromatic discrimination ellipses, which the subjects could not distinguish.

This suggests that the reliability of the ellipse test depends on whether one or more of the measuring directions equally splitting 360° coincide or approach one of the confusion directions. To overcome this, it is recommended to give the confusion directions a prominent role in the preparation of the experimental design, also in the case of the examination of subjects with normal colour vision.

References

[1] B. L. Cole: *Assessment of Inherited Colour Vision Defects in Clinical Practice.* Clin. Exp. Optom., 90/3. (2007)157–175.

[2] M. Gualtieri, C. Feitosa-Santana, M. Lago, M. Nishi, D. F. Ventura: *Early Visual Changes in Diabetic Patients with No Retinopathy, Measured by Color Discrimination and Electroretinography.* Psychol. Neurosci. 6/2. (2013) 227–234.

[3] D. F. Ventura et al.: *Colour Vision and Contrast Sensitivity Losses of Mercury Intoxicated Industry*

Workers in Brazil. Environ. Toxicol. Pharmacol., 19/3, (2005) 523–529.

[4] D. F. Ventura et al.: *Color Vision Loss in Patients Treated with Chloroquine.* Arq. Bras. Oftalmol., 66/5. SUPPL.(2003) 9–15.

[5] G. V Paramei, B. Oakley: *Variation of Color Discrimination across the Life Span.* J. Opt. Soc. Am. A Opt. Image Sci. Vis., 31/4, (2014) A375–A384.

[6] S. Wen: *A Color Difference Metric Based on the Chromaticity Discrimination Ellipses.* Opt. Express, 20/24. (2012) 26441.

[7] D. L. MacAdam: *Uniform Color Scales.* J Opt Soc Am, 64/12, (1974)1691–1702.

[8] Q. Xu, B. Zhao, G. Cui, and M. R. Luo: *Testing Uniform Colour Spaces Using Colour Differences of a Wide Colour Gamut.* Opt. Express, 29/5. (2021) 7778.

[9] S. J. Dain: *Clinical Colour Vision Tests.* Clin. Exp. Optom., 87/4–5. (2004) 276–293.

[10] N. Hasrod, A. Rubin: *Colour Vision: A Review of the Cambridge Colour Test and Other Colour Testing Methods.* African Vis. Eye Heal., 74/1. (2015) 1–7.

[11] M. R. Pointer, G. G. Attridge: *Some Aspects of the Visual Scaling of Large Colour Differences.* Color Res. Appl., 22/5. (1997) 298–307.

[12] S. Abasi, M. Amani Tehran, M. D. Fairchild: *Distance Metrics for Very Large Color Differences.* Color Res. Appl., 45/2. (2020) 208–223.

[13] D. L. MacAdam: *Visual Sensitivities to Color Differences in Daylight.* J. Opt. Soc. Am., 32,/5. (1942) 247–274.

[14] ISO 8586:2012 *Sensory Analysis — General Guidelines for the Selection, Training and Monitoring of Selected Assessors and Expert Sensory Assessors.* 2012. 28.

[15] S. Ishihara: *Tests for Color Blindness.* Tokyo, Kyoto: Kanehara Shuppan Co. Ltd., 1972.

[16] B. C. Regan, J. P. Reffin, J. D. Mollon: *Luminance Noise and the Rapid-Determination of Discrimination Ellipses in Color Deficiency.* Vision Res., 34/10. (1994) 1279–1299.

[17] J. D. Mollon, B. C. Regan: *Handbook of the Cambridge Colour Test.* London, UK, 2000.

[18] B. C. Regan, J. D. Mollon: *Discrimination Ellipses in the MacLeod-Boynton Diagram: Results for Normal and Colour-deficient Subjects Obtained with a CRT Display.* Drum, B. Colour Vis. Defic., XII. (1995) 445–451.

[19] D. F. Ventura et al.: *Preliminary Norms for the Cambridge Colour Test.* In: J. D. Mollon, J. Pokorny, K. Knoblauch: *Normal and Defective Colour Vision*, Eds. Oxford, 2010.

[20] G. V. Paramei: *Color Discrimination across Four Life Decades Assessed by the Cambridge Colour Test.* J. Opt. Soc. Am. A, 29/2. (2012) A290.

[21] M. F. Costa, D. F. Ventura, F. Perazzolo, M. Murakoshi, L. C. D. L. Silveira: *Absence of Binocular Summation, Eye Dominance, and Learning Effects in Color Discrimination.* Vis. Neurosci., 23/3–4. (2006) 461–469.

[22] Á. Urbin, B. V. Nagy: *Chromatic Discrimination Thresholds as a Function of Color Differences and Cone Excitations.* Period. Polytech. Mech. Eng., 65/4. (2021) 385–397.

SZERZŐK JEGYZÉKE
LIST OF AUTHORS